

Theory of the Earth

Don L. Anderson

Chapter 14. Anelasticity

Boston: Blackwell Scientific Publications, c1989

Copyright transferred to the author September 2, 1998.

You are granted permission for individual, educational, research and noncommercial reproduction, distribution, display and performance of this work in any format.

Recommended citation:

Anderson, Don L. Theory of the Earth. Boston: Blackwell Scientific Publications, 1989. <http://resolver.caltech.edu/CaltechBOOK:1989.001>

A scanned image of the entire book may be found at the following persistent URL:

<http://resolver.caltech.edu/CaltechBook:1989.001>

Abstract:

Real materials are not perfectly elastic. Stress and strain are not in phase, and strain is not a single-valued function of stress. Solids creep when a sufficiently high stress is applied, and the strain is a function of time. These phenomena are manifestations of anelasticity. The attenuation of seismic waves with distance and of normal modes with time are examples of anelastic behavior, as is postglacial rebound. Generally, the response of a solid to a stress can be split into an elastic or instantaneous part and an anelastic or time-dependent part. The anelastic part contains information about temperature, stress and the defect nature of the solid. In principle, the attenuation of seismic waves can tell us about such things as dislocation density and defect mobility. These, in turn, are controlled by temperature, pressure, stress and the nature of the lattice defects. If these parameters can be estimated from seismology, they in turn can be used to estimate other anelastic properties such as viscosity. For example, the dislocation density of a crystalline solid is a function of the nonhydrostatic stress. These dislocations respond to an applied oscillatory stress, such as a seismic wave, but they are out of phase because of the finite diffusion time of the atoms around the dislocation. The dependence of attenuation on frequency can yield information about the dislocations. The longer-term motions of these same dislocations in response to a higher tectonic stress gives rise to a solid-state viscosity.

Anelasticity

"As when the massy substance of the Earth quivers."

—CHRISTOPHER MARLOWE, *TAMBURLAINE THE GREAT*

Real materials are not perfectly elastic. Stress and strain are not in phase, and strain is not a single-valued function of stress. Solids creep when a sufficiently high stress is applied, and the strain is a function of time. These phenomena are manifestations of anelasticity. The attenuation of seismic waves with distance and of normal modes with time are examples of anelastic behavior, as is postglacial rebound. Generally, the response of a solid to a stress can be split into an elastic or instantaneous part and an anelastic or time-dependent part. The anelastic part contains information about temperature, stress and the defect nature of the solid. In principle, the attenuation of seismic waves can tell us about such things as dislocation density and defect mobility. These, in turn, are controlled by temperature, pressure, stress and the nature of the lattice defects. If these parameters can be estimated from seismology, they in turn can be used to estimate other anelastic properties such as viscosity. For example, the dislocation density of a crystalline solid is a function of the nonhydrostatic stress. These dislocations respond to an applied oscillatory stress, such as a seismic wave, but they are out of phase because of the finite diffusion time of the atoms around the dislocation. The dependence of attenuation on frequency can yield information about the dislocations. The longer-term motions of these same dislocations in response to a higher tectonic stress gives rise to a solid-state viscosity.

SEISMIC WAVE ATTENUATION

Seismic waves attenuate or decay as they propagate. The rate of attenuation contains information about the anelastic properties of the propagation medium.

A propagating wave can be written

$$A = A_0 \exp i(\omega t - kx)$$

where A is the amplitude, ω the frequency, k the wave number, t is travel time, x is distance and $c = \omega/k$ the phase velocity. If spatial attenuation occurs, then k is complex and

$$A = A_0 \exp i(\omega t - kx) \cdot \exp -k^*x$$

where k and k^* are now the real and imaginary parts of the wave number. k^* is called the spatial attenuation coefficient.

The elastic moduli, say \hat{M} , are now also complex:

$$M = M' + iM''$$

The specific quality factor, a convenient dimensionless measure of dissipation, is

$$Q_M^{-1} = M''/M'$$

This is related to the energy dissipated per cycle $A\varepsilon$:

$$Q = 4\pi\langle\varepsilon\rangle/\Delta\varepsilon$$

where $\langle\varepsilon\rangle$ is the average stored energy (O'Connell and Budyanskiy, 1978). This is commonly approximated as

$$Q = 2\pi\varepsilon_{\max}/\Delta\varepsilon$$

where ε_{\max} is the maximum stored energy. Since phase velocity, c , is

$$c = \frac{\omega}{k} = \sqrt{M/\rho}$$

it follows that

$$Q^{-1} = 2 \frac{k''}{k'} = \frac{M''}{M'} \quad \text{for } Q \gg 1$$

In general $c(\omega)$, $M(\omega)$, $k(\omega)$ and $Q(\omega)$ are all functions of frequency.

For standing waves, or free oscillations, we write a complex frequency, $\omega \pm i\omega^*$, where ω^* is the temporal attenuation coefficient and

$$Q^{-1} = 2 \frac{\omega^*}{\omega}$$

In general, all the elastic moduli are complex, and each wave type has its own Q and velocity. For an isotropic solid the imaginary parts of the bulk modulus and rigidity are denoted as K^* and G^* . Most mechanisms of seismic-wave absorption affect G , the rigidity, more than K , and usually

$$Q_K \gg Q_G$$

Important exceptions over certain frequency ranges have to do with thermoelastic mechanisms and composite systems such as fluid-filled rocks.

Frequency Dependence of Attenuation

In a perfectly elastic homogeneous body, the elastic-wave velocities are independent of frequency. In an imperfectly elastic, or anelastic, body the velocities are dispersive, that is, they depend on frequency. This is important when comparing seismic data taken at different frequencies or when comparing seismic and laboratory data.

A variety of physical processes contribute to attenuation in a crystalline material: motions of point defects, dislocations, grain boundaries and so on. These processes all involve a high-frequency, or unrelaxed, modulus and a low-frequency, or relaxed, modulus. At sufficiently high frequencies the defects, which are characterized by a time constant, do not have time to contribute, and the body behaves as a perfectly elastic body. Attenuation is low and Q is high in the high-frequency limit. At very low frequencies the defects have plenty of time to respond to the applied force and they contribute an additional strain. Because the stress cycle time is long compared to the response time of the defect, stress and strain are in phase and again Q is high. Because of the additional relaxed strain, however, the modulus is low and the relaxed velocity is low. When the frequency is comparable to the characteristic time of the defect, attenuation reaches a maximum, and the wave velocity changes rapidly with frequency.

These characteristics are embodied in the *standard linear solid*, which is composed of a spring and a dashpot (or viscous element) arranged in a parallel circuit, which is then attached to another spring. At high frequencies the second, or series, spring responds to the load, and this spring constant is the effective modulus and controls the total extension. At low frequencies the other spring and dashpot both extend, with a time constant τ characteristic of the dashpot, the total extension is greater, and the effective modulus is therefore lower. This system is sometimes described as a viscoelastic solid.

The Q^{-1} of such a system is

$$Q^{-1}(\omega) = \frac{k_2}{k_1} \frac{\omega\tau}{1 + (\omega\tau)^2}$$

where k_2 and k_1 are, respectively, the spring constants (or moduli) of the series spring and the parallel spring and τ is the relaxation time, $\tau = \eta / k_2$ where η is the viscosity. Clearly, $Q^{-1}(\omega)$ is a maximum, Q_{\max}^{-1} , at $\omega\tau = 1$, and

$$Q^{-1}(\omega) = 2Q_{\max}^{-1} \frac{\omega\tau}{1 + (\omega\tau)^2} \quad (1)$$

and $Q^{-1}(\omega) \rightarrow 0$ as $\omega\tau \rightarrow 0$ and $\omega\tau \rightarrow \infty$ and was $(\omega\tau)^{-1}$ as $\omega \rightarrow 0$. The resulting absorption peak is shown in Figure 14-1.

The phase velocity is approximately given by

$$c(\omega) = c_0 \left(1 + Q_{\max}^{-1} \frac{(\omega\tau)^2}{1 + (\omega\tau)^2} \right) \quad (2)$$

where c_0 is the zero-frequency velocity. The high-frequency or elastic velocity is

$$c_{\infty} = c_0 (1 + Q_{\max}^{-1}) \quad (3)$$

Far away from the absorption peak, the velocity can be written

$$\begin{aligned} c(\omega) &\approx c_0 \left(1 + \frac{1}{2} \frac{k_1}{k_2} Q^{-2} \right) \quad \text{for } \omega\tau \ll 1 \\ &\approx c_{\infty} \left(1 - \frac{k_1^2}{(2k_1 + k_2)k_2} Q^{-2} \right) \quad \text{for } \omega\tau \gg 1 \end{aligned}$$

and the Q effect is only second order. In these limits, velocity is nearly independent of frequency, but Q varies as ω or ω^{-1} . In a dissipative system, Q and c cannot both be independent of frequency, and the velocity depends on the attenuation. When Q is constant, or nearly so, the fractional change in phase velocity is proportional to Q^{-1} rather than Q^{-2} and becomes a first-order effect.

By measuring the variation of velocity or Q in the laboratory as a function of frequency or temperature, the nature of the attenuation and its characteristic or relaxation time, τ , can often be elucidated. For activated processes,

$$\tau = \tau_0 \exp E^*/RT \quad (4)$$

where E^* is an activation energy. Most defect mechanisms at seismic frequencies and mantle temperatures can be described as activated relaxation effects. These include stress-induced diffusion of point and line (dislocation) defects. At very high frequencies and low temperatures, other mechanisms come into play, such as resonances of defects, and these cannot be so described. For activated processes, then,

$$Q^{-1}(\omega) = 2Q_{\max}^{-1} \frac{\omega\tau_0 \exp E^*/RT}{(1 + (\omega\tau_0)^2 \exp 2E^*/RT)} \quad (5)$$

and the relaxation peak can be defined either by changing ω

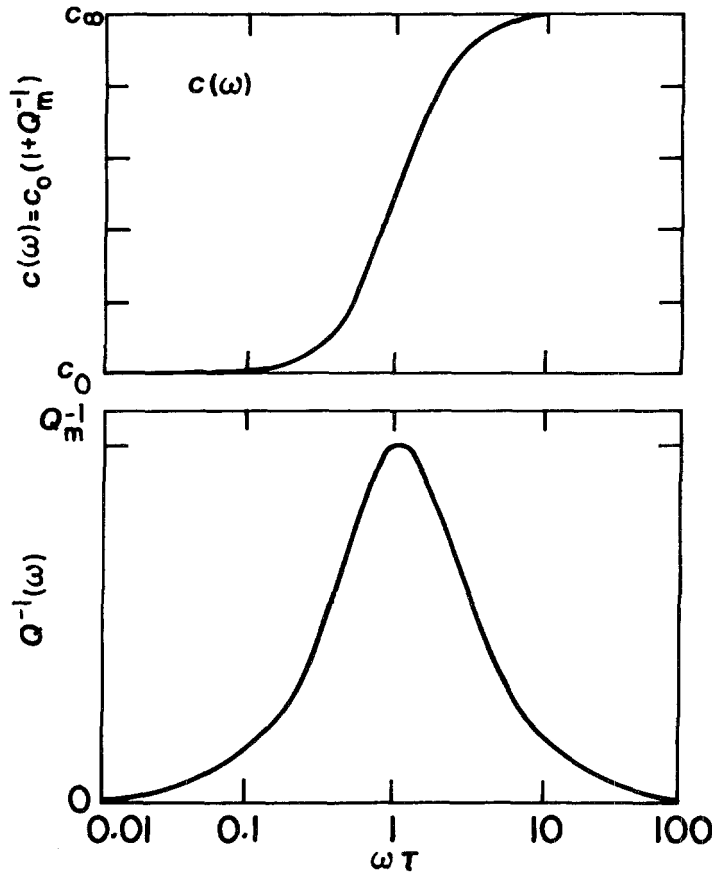


FIGURE 14-1

Specific attenuation function $Q^{-1}(\omega)$ and phase velocity $c(\omega)$ as a function of frequency for a linear viscoelastic solid with a single relaxation time, τ (after Kanamori and Anderson, 1977).

or changing T . Activation energies typically lie in the range of 10 to 100 kcal/mole.

At high temperatures, or low frequencies,

$$Q^{-1}(\omega) = 2Q_{\max}^{-1}\omega\tau_0 \exp E^*/RT \quad (6)$$

This is contrary to the general intuition in the seismological literature that attenuation increases with temperature. However, if τ differs greatly from seismic periods, it is possible that we may be on the low-temperature or high-frequency portion of the absorption peak, and

$$Q^{-1}(\omega) = 2Q_{\max}^{-1} / (\omega\tau_0 \exp E^*/RT), \quad \omega\tau \gg 1 \quad (7)$$

In that case Q does decrease with an increase in T , and in that regime Q increases with frequency. This appears to be the case for short-period waves in the mantle. It is also generally observed that low- Q and low-velocity regions of the upper mantle are in tectonically active and high heat-flow areas. Thus, seismic frequencies appear to be near the high-frequency, low-temperature side of the absorption peak in the Earth's upper mantle. Melting, in fact, may occur before the condition

$$\omega\tau = \omega\tau_0 \exp E^*/RT = 1$$

is satisfied. More generally,

$$\tau = \tau_0 \exp(E^* + PV^*)/RT \quad (8)$$

where V^* , the activation volume, controls the effect of pressure on τ and Q . Because of the pressure and temperature gradient in the mantle, we can expect τ and therefore $Q(\omega)$ to vary with depth. Increasing temperature drives the absorption peak to higher frequencies (characteristic frequencies increase with temperature). Increasing pressure drives the peak to lower frequencies.

Absorption in a medium with a single characteristic frequency gives rise to a bell-shaped Debye peak centered at a frequency $\omega = \tau^{-1}$, as shown in Figure 14-1. The specific dissipation function, Q^{-1} , and phase velocity satisfy the differential equation for the standard linear solid and can be written

$$Q^{-1}(\omega) = 2Q_{\max}^{-1}\omega\tau / (1 + \omega^2\tau^2)$$

$$c^2(\omega) = c_0^2(1 + \omega^2\tau^2 c_\infty^2/c_0^2) / [(1 + \omega^2\tau^2)^2 + 2\omega^2\tau^2 Q_{\max}^{-1}]^{1/2}$$

The high-frequency (c_∞) and low-frequency velocities are related by

$$\frac{c_\infty^2 - c_0^2}{c_0 c_\infty} = 2Q_{\max}^{-1}$$

so that the total dispersion depends on the magnitude of the peak dissipation. For a Q of 200, a typical value for the upper mantle, the total velocity dispersion is 2 percent.

Solids in general, and mantle silicates in particular, are not characterized by a single relaxation time and a single Debye peak. A distribution of relaxation times broadens the peak and gives rise to an absorption band (Figure 14-2). Q can be weakly dependent on frequency in such a band. Seismic Q values are nearly constant with frequency over much of the seismic band. A nearly constant Q can be explained by involving a spectrum of relaxation times and a superposition of elementary relaxation peaks. If τ is distributed continuously between τ_1 and τ_2 (see Anderson and others, 1977), then

$$Q^{-1}(\omega) = (2Q_{\max}^{-1}/\pi) \tan^{-1} [\omega(\tau_1 - \tau_2)/(1 + \omega^2\tau_1\tau_2)]$$

and

$$c(\omega) = c_0(1 + (Q_{\max}^{-1}/2\pi)\ln [(1 + \omega^2\tau_1^2) \div (1 + \omega^2\tau_2^2)])$$

For $\tau_1 \ll \omega^{-1} \ll \tau_2$ the value of Q^{-1} is constant and equal to Q_{\max}^{-1} . The total dispersion in this case is

$$\frac{c_\infty - c_0}{c_0} = (Q_{\max}^{-1}/\pi)\ln(\tau_1/\tau_2)$$

which depends on the ratio τ_1/τ_2 , which is the width of the absorption band. The spread in τ can be due to a distribution of τ_0 or of E^* .

Attenuation Mechanisms

The actual physical mechanism of attenuation in the mantle is uncertain, but it is likely to be a relaxation process involving a distribution of relaxation times. Many of the attenuation mechanisms that have been identified in solids occur at relatively low temperatures and high frequencies and can therefore be eliminated from consideration. These include point-defect and dislocation resonance mechanisms, which typically give absorption peaks at kilohertz and megahertz frequencies at temperatures below about half the melting point. The so-called grain-boundary and cold-work peak and the "high-temperature background" occur at lower frequencies and higher temperatures. These mechanisms involve the stress-induced diffusion of dislocations. The Bordoni peak occurs at relatively low temperature in cold-worked metals but may be a higher-temperature peak in silicates. It is apparently due to the motion of dislocations since it disappears upon annealing.

Even in the laboratory it is often difficult to identify the mechanism of a given absorption peak. The effects of amplitude, frequency, temperature, irradiation, annealing, deformation and impurity content must be studied before the mechanism can be identified with certainty. This information is not available for the mantle or even for the silicates that may be components of the mantle. Nevertheless, there is some information which helps constrain the possible mechanism of attenuation in the mantle.

1. The frequency dependence of Q is weak over most of the seismic band. At frequencies greater than about 1 Hz, Q appears to increase linearly with frequency. This is consistent with the behavior expected on the low-temperature side of a relaxation band. A weak frequency dependence is best explained by invoking a distribution of relaxation times. A distribution of dislocation lengths, grain sizes and activation energies may be involved.
2. Although it has not been specifically studied, there has been no evidence brought forward to suggest that seismic attenuation is amplitude or stress dependent. Laboratory measurements of attenuation are independent of amplitude at strains less than 10^{-6} . Strains associated with seismic waves are generally much less than this.
3. The radial and lateral variations of Q in the mantle are our best clues to the effects of temperature and pressure. The lower- Q regions of the mantle are in those areas where the temperatures are highest. This suggests that most of the upper mantle is on the low-temperature side of an absorption band or in the band itself. At a depth of 100 km the temperature of the continental lithosphere is about 200 K less than under oceans. Q is roughly 7 times larger under continents. This implies an activation energy of about 50 kcal/mole.
4. The variation of Q with depth in the mantle covers a range of less than two orders of magnitude. This means that the effects of temperature and pressure are relatively modest or that they tend to compensate each other.
5. Losses in shear are more important than losses in compression. This is consistent with stress-induced motion of defects rather than a thermoelastic mechanism or other mechanisms involving bulk dissipation.

Spectrum of Relaxation Times

Relaxation mechanisms lead to an internal friction peak of the form

$$Q^{-1}(\omega) = \Delta \int_{-\infty}^{\infty} D(\tau)[\omega\tau/(1 + \omega^2\tau^2)] d\tau \quad (9)$$

where ω is the applied frequency, τ is a characteristic time, $D(\tau)$ is called the retardation spectrum and Δ is the modulus defect $(G_\infty - G_r)/G_r$, the relative difference between the high-frequency, unrelaxed shear modulus G_∞ , and the low-frequency, relaxed modulus G_r . The modulus defect is also a measure of the total reduction in modulus that is obtained in going from low temperature to high temperature. For a dislocation model the modulus defect is due to the strain contributed by dislocation bowing. The dislocations bow to an equilibrium radius of curvature that is dictated by the applied stress. The rate at which they do so is controlled by the propagation of kinks or diffusion of point defects near

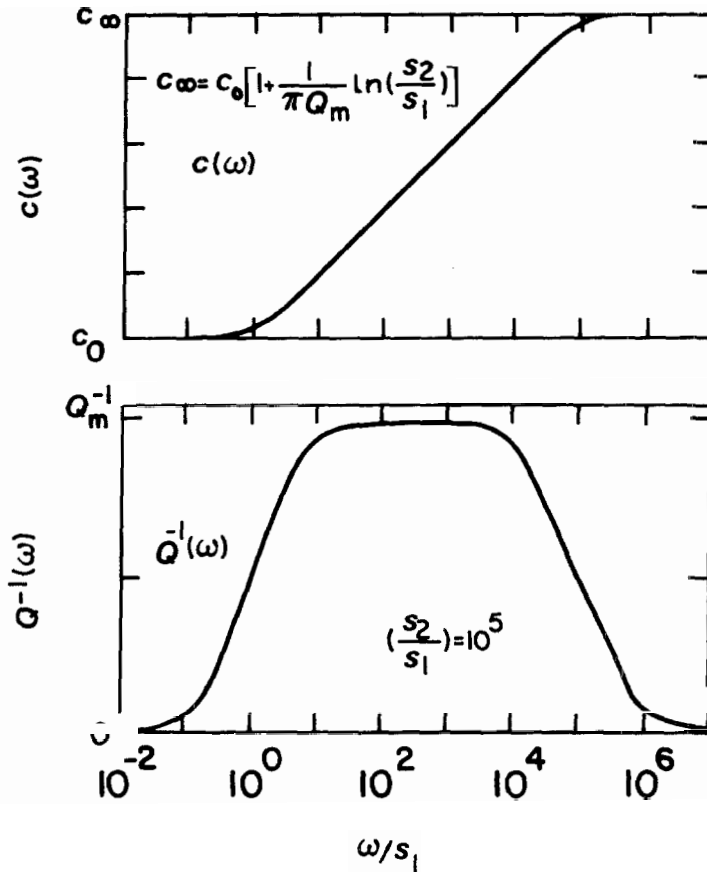


FIGURE 14-2

Band-limited constant-Q model with cutoff frequencies s_1 and s_2 ($s = 1/\tau$) (after Kanamori and Anderson, 1977).

the dislocation and therefore is an exponential function of temperature.

A convenient form of the retardation spectrum is

$$D(\tau) = [\alpha/(\tau_2^\alpha - \tau_1^\alpha)]\tau^{\alpha-1} \quad (10)$$

for $\tau_1 < \tau < \tau_2$ and zero elsewhere (Minster and Anderson, 1981). τ_1 and τ_2 are the shortest and longest relaxation times, respectively, of the mechanism being considered.

When $\tau_1 \approx \tau_2$, equation 9 reduces to the well-known Debye peak. When $a = 0$ and $\tau_2 \gg \tau \gg \tau_1$, a frequency-independent Q results. The more general case of $0 < \alpha < 1$ has been discussed by Anderson and Minster (1979, 1980). This leads to a weak dependence, $Q(\omega) \approx \omega^\alpha$, for $\tau_1 < \tau < \tau_2$ and has characteristics similar to Jeffreys' (1970) modification of Lomnitz's law. Outside the absorption band, $Q(\omega) \approx \omega^{\pm 1}$ for $\omega\tau \gg 1$; this result holds for all relaxation mechanisms.

The Q corresponding to frequencies ω such that

$$\omega\tau_1 \ll 1 \ll \omega\tau_2$$

is given by

$$Q(\omega) = \cot \frac{a\pi}{2} + \frac{2J_u}{\pi\alpha\delta J}$$

$$\times [(\omega\tau_2)^\alpha - (\omega\tau_1)^\alpha] \cos \frac{\alpha\pi}{2}$$

$$\approx \frac{2J_u}{\pi\alpha\delta J} (\omega\tau_2)^\alpha \cos \frac{a\pi}{2} \quad (11)$$

since $\tau_2 \gg \tau_1$ and $\cot \alpha\pi/2$ is small. J_u , J_r , and $\delta J = J_r - J_u$ are the unrelaxed, relaxed, and defect compliances, respectively. The compliance is strain divided by stress.

For high frequencies, $1 \ll \omega\tau_1 \ll \omega\tau_2$,

$$Q(\omega) = (1 - \alpha)(J_u/\alpha\delta J)(\tau_2/\tau_1)\alpha(\omega\tau_1)$$

At low frequencies,

$$Q(\omega) = (1 + \alpha)(J_r/\alpha\delta J)(\omega\tau_2)^{-1}$$

For a thermally activated process the characteristic times depend on temperature. It is clear that at very low temperature the characteristic times are long and $Q \propto \omega$. At very high temperature, Q is predicted to increase as ω^{-1} . Equation 11 holds for intermediate temperatures.

The dispersion appropriate for the frequency-dependent Q model considered above gives, in the case $Q \gg 1$,

$$G_1/G_2 = 1 - \cot(\alpha\pi/2)(\omega_2/\omega_1)Q_2^{-1}$$

where Q_2 is the Q at ω_2 . The rigidities at the two frequen-

cies are $G_1(\omega_1)$ and $G_2(\omega_2)$. This applies for $\omega\tau < \omega\tau_2$. For low frequencies, $G = G_r$. For high frequencies, $G = G_u$. For simple dislocation networks the difference between the relaxed and unrelaxed moduli is about 8 percent (Minster and Anderson, 1981).

ACTIVATED PROCESSES

For simple point-defect mechanisms τ_o^{-1} is close to the Debye frequency, about 10^{13} Hz. For mechanisms involving dislocations or dislocation-point defect interactions, τ_o depends on other parameters such as dislocation lengths, Burger's vectors, kink and jog separations, Peierls stress, and interstitial concentrations. The activation energy, depending on the mechanism, is a composite of activation energies relating to self-diffusion, kink or jog formation, Peierls energy, bonding energy of point defects to the dislocation, core-diffusion and so on. E^* for creep of metals is often just the self-diffusion activation energy, E_{SD} .

Nonelastic processes in geophysics are commonly expressed in terms of viscosity, for long-term phenomena, and Q , for oscillatory and short-term phenomena. It is convenient to express these in terms of the characteristic time. For creep,

$$\tau = \sigma/G\dot{\epsilon} = \eta/G$$

where σ , G , $\dot{\epsilon}$ and η are the deviatoric stress, rigidity, strain rate and viscosity, respectively. Thus, the characteristic time can be simply computed from creep theories and experiments.

Relaxation theories of attenuation can be described by $Q(\omega\tau)$. In the mantle, where Q is low, we infer that the characteristic relaxation time is close to $1/\omega$, the reciprocal of the measurement frequency. High values of Q indicate that $\omega \gg 1/\tau$ or $\omega \ll 1/\tau$. In these cases $Q \approx \omega$ or ω^{-1} . When Q is slowly varying we are probably in the midst of an absorption band that is conveniently explained as a result of a distribution of relaxation time.

Since Q is small in the higher-temperature regions of the mantle, it is likely that at seismic periods the mantle is on the low-temperature side of an absorption band. Thus

$$Q^{-1} = 2Q_{\max}^{-1}/\omega\tau = (2Q_{\max}^{-1}/\omega\tau_o)\exp(-E^*/RT) \quad (12)$$

in regions of rapidly varying attenuation. The seismic data can be used to estimate the relaxation time in the upper mantle and its variation with depth. The high-temperature background (HTB) is a dominant mechanism of attenuation in crystalline solids at high temperature and low frequency. This usually satisfies a $Q \approx \omega$ or $Q \approx \omega^\alpha$ relation. This can be interpreted in terms of a distribution of relaxation times. The former is valid for all relaxation mechanisms when the measurement frequency is sufficiently high. In the following τ will be used for the pre-exponential creep, or Max-

well, relaxation time and τ_o will be used for the attenuation, or Q , characteristic time.

Activation Energies for Climb and Glide

The creep of ductile materials such as metals is rate-limited by self-diffusion. This is the case for either pure diffusional creep or dislocation climb. In these circumstances the activation energy for creep is the same as that for self-diffusion. In olivine the activation energy for creep is appreciably higher than that for self-diffusion of O^{2-} or Si^{4+} . This suggests that creep may be controlled by kink or jog formation.

Kinks are offsets in a dislocation line in the glide plane off a crystal. Kinks separate portions of a dislocation that are in adjacent potential valleys, separated by a Peierls energy hill. Segments of a dislocation line that are normal to the glide plane are called jogs. At finite temperature, dislocations contain equilibrium concentrations of kinks and jogs. The kinks and jogs undergo a diffusive drift under an applied stress, producing glide and climb, respectively.

The activation energy for creep when dislocation climb is due to nucleation and lateral drift of jogs is $(1/2)(E_{SD}^* + 2E_j^*)$ or $(1/2)(E_k^* + E_{CD}^* + 4E_j^*)$, depending on whether the dislocations are longer or shorter than the equilibrium jog spacing. Here E_k^* , E_{CD}^* and E_j^* are the activation energies for self-diffusion, core diffusion and jog formation, respectively (Hirth and Lothe, 1968).

E_{SD}^* is 90 kcal/mole for both oxygen and silicon diffusion in olivine (Jaoul and others, 1979). The jog formation energy is somewhat greater than kink formation energy (Hirth and Lothe, 1968). The activation energy controlling high-temperature deformation of olivine has been estimated to be 135 kcal/mole from the climb of dislocation loops in olivine (Kohlstedt and Goetze, 1974; Kohlstedt, 1979) and 122–128 kcal/mole from creep data on olivine (Goetze and Brace, 1972; Goetze, 1978).

In the absence of interstitial defects near the dislocation, the activation energy for glide is E_k^* if the kink density is high and $2E_k^*$ when the dislocation length is shorter than the equilibrium distance between kinks. E_k^* is the kink formation energy, which is about 26 kcal/mole (Ashby and Verall, 1978). The activation energy for glide is therefore 52 kcal/mole if the kink spacing is large or if double kink formation is required for glide. If point defects must diffuse with the dislocation line, then their diffusivity may be rate limiting. The activation energy for Mg-Fe interdiffusion in olivine is about 50–58 kcal/mole (Misener, 1974). Dislocation glide in olivine will therefore probably have an activation energy of the order of 50–60 kcal/mole, unless there are slower-moving species in the vicinity of the dislocation. Olivine in contact with pyroxene is likely to have excess silicon interstitials as a dominant point defect. The activation energy in this case may be due to drag of silicon interstitial—about 90 kcal/mole. There is also a small term

TABLE 14-1
Material Properties for Olivine

Property	Symbol	Value	Units
Burger's vector	b	6×10^{-8}	cm
Oxygen ion volume	Ω	1×10^{-23}	cm ³
Shear modulus	G	8×10^{11}	dy/cm ²
Silicon diffusivity			
Pre-exponential	D_{Si}	1.5×10^{-6}	cm ² /s
Activation energy	E_{Si}	90	kcal/mole
Oxygen diffusivity			
Pre-exponential	D_{ox}	3.5×10^{-3}	cm ² /s
Activation energy	E_{ox}	89	kcal/mole
Mg-Fe diffusivity			
Pre-exponential	D_{Mg}	3.4×10^{-3}	cm ² /s
Activation energy	E_{Mg}	47	kcal/mole
Subgrain size \div			
Dislocation length	K'	15	—
Kink energy	E_k	26	kcal/mole
Jog energy	E_j	35	kcal/mole

Ashby and Verall (1978).

representing the binding energy of interstitials to the dislocation. This is ordinarily a few kilocalories per mole, but data are lacking for silicates. The kink and jog formation energies in silicates are also highly uncertain, and the above estimates for olivine are approximate.

Point defects can also diffuse along the core of a dislocation. The activation energy for dislocation core diffusion should be similar to that for surface diffusion. This, for metals, is usually about $\frac{1}{2}$ to $\frac{2}{3}$ of the lattice diffusion value. If this rule applies to olivine, the core diffusion activation energy would be about 50 to 60 kcal/mole. High values for the core and surface activation energies are expected from the heat of vaporization, which is much higher for silicates than for metals. If we adopt $E_{SD}^* = E_{CD}^* = 90$ kcal/mole and $E_{creep}^* = 125$ kcal/mole, then the implied jog formation energy is 35 kcal/mole. This is much greater than is typical of metals. It is also expected, since the kink and jog formation energies are proportional to Gb^3 , which is much greater for silicates than for metals.

Because of the high values for core diffusion and jog formation, we expect relatively high values for the creep activation energy for silicates and for a non-correspondence with the self-diffusional activation energy, except for very small grain sizes and low stresses, where diffusional creep may be important.

A summary of the physical properties of olivine is assembled in Table 14-1. These will be used in subsequent calculations.

Geophysical Constraints on the Activation Parameters

Some of the activation parameters for creep and attenuation can be estimated directly from geophysical data. The characteristic time scales of relaxation processes in the mantle depend on temperature, through the activation energy, and on the pressure, through the activation volume. Stress has an indirect effect on relaxation times since it controls such parameters as dislocation density and subgrain size. The characteristic frequencies of atomic processes and processes involving dislocation motions are typically 10^{10} to 10^{13} Hz. The characteristic relaxation time for creep in the upper mantle, the ratio of viscosity to rigidity, is about 10^{10} s. For temperatures of 1500–1600 K, appropriate for the upper mantle, the required activation energy is 145–170 kcal/mole. This is similar to the activation energy for creep of olivine and values inferred for the climb of dislocations in olivine (Goetz and Kohlstedt, 1973).

Judging from the attenuation of surface waves, the characteristic time controlling the attenuation of seismic waves in the upper mantle is of the order of 100 s. This implies an activation energy in the range 90–100 kcal/mole for the above τ_0 . This is close to the activation energy found for diffusion of O^{2-} and Si^{4+} in olivine (Table 14-1). A higher value for τ_0 gives a smaller value for E^* .

The trade-off between τ_0 and E^* is shown in Figure 14-3. The curves to the right cover a range of estimated

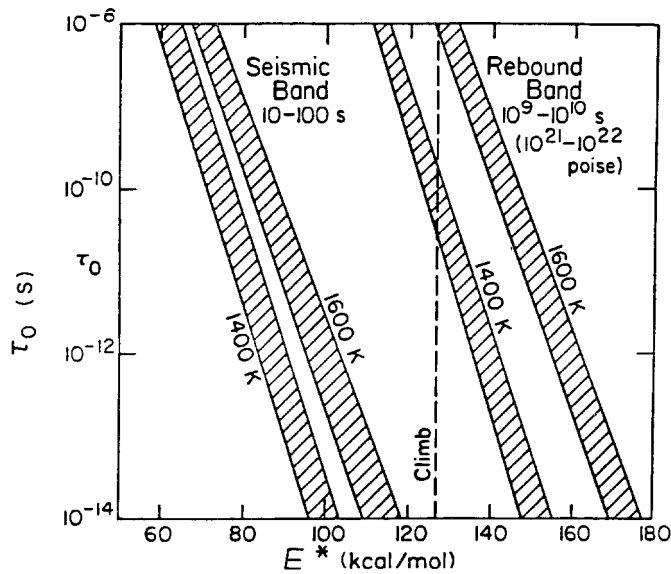


FIGURE 14-3

τ_0 versus activation energy combinations that satisfy the seismic data (left) and rebound data (right) for a range of upper-mantle temperature. The dashed line is the expected activation energy for dislocation climb in olivine (Anderson and Minster, 1980).

upper-mantle temperatures and viscosities. The curves to the left represent the seismic band. Theories of creep and attenuation predict τ_0 - E^* pairs. Those that fall in the areas shown are geophysically plausible mechanisms. Low values of τ_0 require low values for E^* . The characteristic pre-exponential times are not the same for creep and attenuation.

It is not simple to estimate the pre-exponential characteristic time appropriate for attenuation in the mantle. High-temperature background damping processes in metals give τ_0 in the range of 10^{-12} - 10^{-14} s (Woigard, 1976). Lower temperature peaks give characteristic times one or two orders of magnitude larger. Theoretically, the times scale as the diffusivity, which is typically three orders of magnitude lower in silicates than in metals. On the other hand, subgrain sizes and dislocation lengths in the mantle can be expected to be one or two orders of magnitude greater than typical laboratory grain sizes in metals. Since $\tau_0 \approx l^2/D$, the characteristic time for the mantle may therefore be of the order of 10^{-6} to 10^{-8} s. There are very few data on silicates. The relaxation times have been estimated from forsterite data as about 10^{-8} s (Jackson, 1969). This implies an activation energy of 58-74 kcal/mole if the upper-mantle seismic absorption band is centered at 100 s.

Although τ is proportional to l^2 for most attenuation and creep mechanisms, there are other factors that affect the characteristic times. Steady-state creep is controlled by self-diffusion of the slowest moving species. This affects both D , and E^* . E^* for creep, which also includes the energy of

jog formation, is therefore greater than E^* for attenuation, which need not involve self-diffusion. For a polygonized network the climb of dislocations in cell walls is rate-limiting, but the characteristic time for creep involves both the motion of the long mobile dislocations in the cells and the shorter dislocations in the walls. For attenuation, the separate population of dislocations would give rise to widely separated internal friction peaks. A wide separation of characteristic times can therefore be obtained from a single dislocated solid.

Experiments on dislocated single crystals of silicates are needed to isolate the attenuation mechanisms in the mantle. Some of the theoretical predictions of this chapter have been confirmed by experiments on rocks (Berckhemer and others, 1979, 1982; Kampfmann and Berckhemer, 1985). The effects of partial melting are evident in these data.

Estimates of τ_0 and E^* for Olivine

The characteristic relaxation time for creep of olivine can be obtained from high-temperature laboratory experiments:

$$\dot{\epsilon} = A\sigma^n \exp(-E^*/RT)$$

Using the Kohlstedt-Goetze (1974) data with $n = 3$ and $E^* = 125$ kcal/mole and the relation

$$\hat{\tau}_0 = \sigma G / \dot{\epsilon}_0$$

we obtain $\hat{\tau}_0 = 3 \times 10^{-9}$ s for a stress of 10 bars. The low-stress data have a σ^2 trend. In this case $\hat{\tau}_0$ is 10^{-9} s.

From the seismic rigidity and the postglacial rebound viscosity, the relaxation time of the upper mantle is $10^{10 \pm 1}$ s. Using an activation energy of 125 kcal/mole and a range of upper-mantle temperatures from 1100 to 1300°C, the inferred value for $\hat{\tau}_0$ is 10^{-6} to 10^{-10} s. This is consistent with the laboratory creep data for differential stresses in the range of a fraction of a bar to about 5 bars. The mantle $\hat{\tau}_0$ values also overlap the lower values for $\hat{\tau}_0$ determined from dislocation mechanisms rate-limited by silicon diffusion.

The effect of pressure can be estimated from the observation that both viscosity and Q do not vary by more than two orders of magnitude in the mantle. This constrains the activation volume to be between 4 and 9 cm³/mole. Since the activation volume of oxygen, the largest major ion in the mantle, is about 11 cm³/mole and decreases with pressure, and since the effective activation volume depends on all diffusing ions for coupled diffusion, the result from the mantle is consistent with diffusional control for both dislocation creep and attenuation.

A crude estimate of the activation energy controlling attenuation can be obtained from the observation that Q can vary by about an order of magnitude over relatively short distances both laterally and vertically in the upper mantle. Using 200°C as a reasonable difference in temperature, the inferred activation energy is about 52 kcal/mole. This, in

turn, requires a τ_0 of about 10^{-5} – 10^{-6} s for the attenuation mechanism.

These results support previous conclusions that both creep and attenuation in the mantle are activated processes that are controlled by diffusion. They are also consistent with numerous studies on a variety of materials finding that high-temperature creep and internal friction are controlled by the diffusive motion of dislocations. The large modulus defect implied by the upper-mantle low-velocity, low-Q zone is also consistent with a dislocation relaxation mechanism, perhaps aided by partial melting. Point-defect internal friction peaks are generally relatively sharp, occur at low temperatures and do not exhibit the low Q's and large velocity dispersion that characterize the mantle and the high-temperature internal friction peaks.

Although attenuation and creep, or viscosity, are different mechanisms, they are both activated processes that depend strongly on temperature, pressure and defect concentrations. We therefore expect the low-Q region of the upper mantle to be a low-viscosity region (Anderson, 1966). By the same reasoning we expect the lower mantle to exhibit high viscosity. High pressure decreases the mobility of point defects, leading to high viscosity and longer relaxation times. Parts of D" may have high thermal gradients, and viscosity may decrease in these regions.

The high viscosity of the lower mantle, expected from both Q and ΔV^* considerations, probably means that lower mantle convection is more sluggish than that associated with plate tectonics.

DISLOCATION DAMPING

The passage of a stress wave through a crystalline solid can cause a stress-induced diffusive motion and reordering of such point defects as vacancies, interstitial or solute impurity atoms, and substitutional atoms. This reordering can take place in a single crystal if the point defect produces distortions that have a lower symmetry than that of the lattice. In polycrystals defects undergo a mass transport between regions of different dilatational strain. A characteristic feature of atomic diffusion is the relatively long time of relaxation and its strong dependence on temperature. The relaxation time for the process is of the order of the inverse jumping frequency of the defect. This frequency, ω_R , depends on the temperature as

$$\omega_R = \omega_0 e^{E^*/RT}$$

where E^* is an energy of activation and R is the gas constant. The activation energies for elements in metals are of the order of tens of kilocalories per mole. For very rapid varying stresses or for very low temperatures, the defects do not have a chance to move, and stress and strain are in phase and no losses occur. For very slowly varying stresses or for very high temperatures, the diffusion frequency

can be greater than the applied frequency, again giving no delay and no loss. For intermediate frequencies and temperatures the motion of defects is out of phase with the applied stress, and a typical relaxation peak occurs. Point-defect attenuation mechanisms occur at much higher frequencies than seismic-wave frequencies and, acting alone, are negligible in seismic problems. However, point defects interacting with dislocations may be important in seismic-wave attenuation.

Dislocations play a significant role in both the plastic behavior and damping properties of single crystals. They are also involved in the properties of polycrystalline substances. There are basically three kinds of mechanical losses that are associated with dislocations: hysteresis, resonance, and relaxation losses. Some dislocation mechanisms give rise to damping that is independent of amplitude and varies with frequency; other mechanisms depend on the amplitude of the stress wave and vary only slowly with frequency. The decrement and modulus changes due to dislocation motions depend on the orientation of the crystal since only the shear component of an applied stress in the slip direction contributes to dislocation motion.

The motion of dislocations that are pinned down by impurities or other dislocations is a common loss mechanism in metal single crystals. The damping depends sensitively on the amount of previous cold work and on the purity of the metal. Increasing the number of impurity atoms or increasing the number of dislocations by cold work provides more anchoring points, and the internal friction decreases. Decreases in internal friction are accompanied by increases in the elastic moduli. The pinning of dislocations by point defects is especially effective at low temperatures and high frequencies since the ability of an impurity atom to follow an alternating stress is controlled by the slow process of diffusion. Amplitude dependence is attributed to the breakaway of the dislocation line from the impurity atoms at large strain amplitudes.

The name hysteresis is given to losses associated with the occurrence of irreversible changes of state. Typical of hysteresis are those in which dislocations are irreversibly torn away from pinning points, such as impurity atoms or other point defects. This mechanism is frequency independent and depends on the amplitude of applied stress. It is suppressed by annealing, by increasing the impurity concentration or by irradiation with neutrons or fast electrons, all of which serve to more effectively pin the dislocation and prevent breakaway. The binding energy of an impurity atom to a dislocation is rather small, and, therefore, the dependence of hysteresis damping on temperature is rather small.

Resonance motion of dislocations within their equilibrium potential valleys can contribute to the damping of waves with frequencies comparable to the resonant frequency of the pinned dislocation segment. Because of the presumed shortness of dislocation loops, this will be impor-

tant only at high frequencies, say megahertz. Therefore, we concentrate on relaxation, or diffusional, processes.

The general expression for the characteristic time of stress-induced diffusion of a dislocation line is

$$\tau = (kTL^2/D_oGb^3) \exp(E^*/RT)$$

(Hirth and Lothe, 1968). In the bowed-string approximation for climb, L is the dislocation length, D_o is the pre-exponential self-diffusion coefficient, E^* is the activation energy for self-diffusion (SD) and b is the Burger's vector. If the climb is rate-limited by core diffusion (CD), then

$$L^2 = l^2/\lambda b$$

where l is the dislocation length, $\lambda = b \exp(E_j/RT)$ is the jog separation and D_o and E^* refer to core diffusion. The effective activation energy is therefore the sum of the core diffusion and jog formation energies. If $D_o(\text{CD}) = 10^3 D_o(\text{SD})$ and $l = 10^3 b$, the τ_o for core diffusion is 10^3 times that for self-diffusion. At modest temperature, however, $\tau(\text{CD}) < \tau(\text{SD})$ if $E_{\text{CD}} < E_{\text{SD}}$. In general, relaxation peaks with high activation energies occur at higher temperature and lower frequency than those with lower activation energies. The presence of point defects, kinks or jogs along the dislocation line changes the characteristic time.

An estimate of the relaxation time for climb can be obtained by assuming that the dislocation length equals the subgrain size, which in turn is related to the tectonic stress

$$L = 15Gb/\sigma$$

Using D_{Si} and σ between 1 and 10 bars we obtain τ_o of $1-10^{-2}$ s. Neither the self-diffusion nor the core-diffusion characteristic times can be brought into the upper-mantle seismic band with the appropriate activation energy. The actual mobile dislocation lengths may be an order of magnitude smaller than the subgrain size. With an activation energy of 90 kcal/mole the relaxation time at upper mantle temperatures is 10^8 to 10^6 s, still well outside the seismic band but straddling the Chandler period. Dislocation climb in subgrains is therefore unlikely to contribute to seismic attenuation but may contribute to damping of the Chandler wobble.

The dislocation lengths in cell walls are an order of magnitude smaller than in the cells. This makes a further reduction in τ_o to about 10^{-5} to 10^{-7} s, which gives relaxation times just outside the seismic band at mantle temperatures and $E^* = 90$ kcal/mole, but the relaxation strength is very small because of the limited bow-out possible for small dislocations. Therefore, it appears that dislocation climb, an important mechanism of steady-state creep, can be ruled out as a mechanism for attenuation in the mantle. We therefore turn our attention to dislocation glide.

In general, dislocations glide much faster than they climb, and the relaxation time is therefore much reduced. Glide is rate-limited by lattice (Peierls) stresses or by point

defects. For a gliding dislocation, rate-limited by the diffusion of interstitial defects,

$$L^2 = C_i l^2$$

where C_i is the concentration of interstitials along the dislocation line at sufficiently high temperature,

$$C_i = C_D \exp(-E_B/RT)$$

and C_D is the bulk concentration of interstitial point defects or impurity atoms and E_B is the binding energy of the point defects to the dislocation line. The diffusivity is that appropriate for the diffusion of the impurity or interstitial ions.

Using $D_o = 10^{-3}$ cm²/s and $C_D \approx C_i = 10^{-3}$, we obtain τ_o of 10^{-6} to 10^{-8} s for typical dislocation lengths appropriate for mantle stresses of 1 to 10 bars. These, combined with activation energies appropriate for diffusion of cations in silicates, give relaxation times in the seismic band at upper-mantle temperatures. The impurity content refers to that in the subgrains. Most impurities in the mantle are probably at grain boundaries, and therefore the grain interiors are relatively pure. The above estimate for C_D is therefore not unreasonable.

The relaxation strength is given by

$$2Q_{\text{max}}^{-1} = (1/6 \sqrt{5}) \rho_m l^2$$

for a collection of randomly oriented gliding dislocations (Minster and Anderson, 1981). In the subgrains $\rho_m = 1/l^2$ for a rectangular grid of dislocations, and the relaxation strength is about 7.5 percent for a Q of about 26. The same relationship holds for a dislocation network in the cell walls, but because of the small volume in the walls the average relaxation strength is very small for the wall contribution to the attenuation. The relaxation strength is proportional to the area swept out by the gliding dislocations and gives the difference between the high-frequency or low-temperature modulus and the relaxed modulus.

The Koster peak occurs in cold-worked metals containing interstitial impurities, some of which have concentrated along the dislocations. It occurs at high temperature and low frequency and usually gives a τ_o of 10^{-13} to 10^{-14} s for metals with oxygen, nitrogen or hydrogen interstitials. It is believed to be caused by an interaction between dislocations and interstitial point defects in the neighborhood of the dislocation. With reasonable choices of parameters, this type of mechanism can explain attenuation in the mantle.

The grain-boundary peak (GBP) occurs in metals at about one-half the melting temperature at 1 Hz; actually, several peaks are often observed between about 0.3 and 0.6 of melting temperature. The activation energies range from about 0.5 to 1.0 times the self-diffusion activation energy and are higher for the high-temperature peaks. An increase in solute concentration increases the magnitude of the higher temperature peak (Woigard, 1976). These peaks are all superimposed on an even stronger high-temperature

background (HTB) which dominates at very high temperature. In synthetic forsterite a strong peak occurs at about 0.25–0.5 Hz at 1000°C (Berckhemer and others, 1982) with an activation energy of 57 kcal/mole. At upper-mantle temperatures this absorption would shift to about 10^{-2} s and therefore would not be important at seismic frequencies. In addition the peak is much less pronounced in natural olivine, and the HTB gives greater absorption than the GBP at temperatures greater than about 1500°C. The GBP may be responsible for attenuation in the lithosphere.

The Bordoni peak was first identified in deformed (cold-worked) metals at low temperature. It is unlikely to be important at mantle temperatures and seismic frequencies, but it would be useful to know its properties for mantle minerals since it contains information about the Peierls energy. The Hirth and Lothe (1968) theory for the characteristic relaxation time gives

$$\tau = \frac{b^2 kT}{2E_k D_k} \exp(2E_k/RT)$$

With nominal values for olivine the relaxation time at mantle temperatures is 10^{-7} s, thus this is a high-frequency, low-temperature mechanism. The controlling activation energy is $2E_k$ or about 52 kcal/mole for olivine. This combination of τ_0 and E^* make it unlikely that the Peierls energy alone controls attenuation in the mantle. It may be responsible for the "grain boundary" peak in olivine, for which Jackson (1969) obtained τ_0 of 10^{-13} s and E^* of 57 kcal/mole. The value for E_k , however, is uncertain.

Values of $\hat{\tau}_0$ of order 10^{-7} to 10^{-12} s for the upper mantle are implied by relaxation times of 10^9 – 10^{10} s at temperatures of 1400–1600 K and an activation energy of 12.5 ± 5 kcal/mole. These values are consistent with both laboratory creep data and creep in a polygonized network model of olivine if the stresses are less than about 10 bars. If kilobar-level stresses existed in the upper mantle, then the inferred viscosity and relaxation times would be at least six orders of magnitude lower than observed. On the other hand, there is no contradiction with kilobar-level stresses being maintained in the lithosphere for 10^6 years if temperatures are less than about 900 K. Kilobar-level stresses also shift the absorption band to much higher frequencies because of the high dislocation density and short dislocations, or small grains, at high stress.

The same dislocations contribute to phenomena with quite different time scales. The climb of jogged dislocations is rate-limited by self-diffusion and jog nucleation. In silicates, and other materials with high Peierls energy, the activation energy for creep can be appreciably greater than for self-diffusion. At finite temperature the creep rate will therefore be slower, and the characteristic time longer, than for materials rate-limited by self-diffusion alone. The effective activation energy for creep is either E_j or $2E_j$ times greater than for self-diffusion, depending on whether the

dislocation length is smaller or greater than the equilibrium spacing of thermal jogs. These two situations lead to a σ^{-3} or σ^{-2} creep law (Hirth and Lothe, 1968). If the activation energy for core diffusion is less than for self-diffusion, the effective activation energy is reduced by one-half the difference of the two. This is a relatively small effect and appears to be negligible for olivine.

On the other hand, the glide of dislocations is controlled by a much smaller activation energy and is therefore much faster than climb at finite temperature. This is the case whether glide is controlled by kink nucleation or diffusion of interstitials. Both creep and attenuation depend on dislocation length and therefore tectonic stress. They are both also exponentially dependent on temperature although the controlling activation energies are different. In principle, the viscosity and stress state of the mantle can be estimated from the seismic Q .

Grain-boundary Losses

In addition to thermoelastic and scattering losses associated with grain boundaries in polycrystals, there are relaxation effects related to the dislocation mechanism at grain boundaries. Boundaries between grains of different orientation or composition are regions of vacancies, impurities, high strain, general disorder and, at high temperatures, partial melting. Losses associated with grain boundaries are high compared to other processes. The simplest kind of grain boundary is simply a plane separating slightly misoriented crystals. Such a boundary can be considered to be a series of edge dislocations that can be made to glide or to migrate upon the application of a shearing stress.

More complicated boundaries can migrate by diffusion of atoms if the temperature is high enough to overcome the activation energy of diffusion. As in other relaxation mechanisms, the temperature of the maximum attenuation shifts as the driving frequency is changed. For high-frequency vibrations, when the relaxation of stress by diffusion cannot keep up with the applied stress, the internal friction increases with temperature and with the grain-boundary area per unit volume, that is, inversely with grain size.

The energy dissipated across a slip boundary is proportional to the product of relative displacement and shear stress. At low temperatures relative displacement between grains is small, and at high temperatures the shear stress across boundaries is essentially relaxed at all times. Appreciable energy dissipation by grain-boundary slip occurs only at intermediate temperatures where there is both displacement and shear stress between grains.

Grain-boundary damping was initially attributed to sliding at grain boundaries, which relaxed the shear stress across the boundary. The boundary was interpreted as a region of disorder that would behave as a film of viscous fluid. The activation energy measured for grain-boundary

damping, however, shows good correlation with values measured for grain-boundary diffusion and creep. This suggests that the grain-boundary "sliding" is actually due to ordering and reordering of atoms under a stress bias in the boundary by diffusion. Representative values for the activation energies associated with grain-boundary damping are 46 kcal/mole for iron and 22 kcal/mole for silver; these are close to measured values for grain-boundary diffusion. At low stress levels a stress-induced migration of arrays of dislocations by dislocation climb is probably a more appropriate description of grain-boundary losses than is grain-boundary sliding. This climb would be controlled by self-diffusion rates in the boundary region.

Although grain-boundary damping is clearly an activated process, the laboratory peaks are too broad to be fit by a unique value for the relaxation time, even in pure substances. A range of activation energies is indicated. The differences in orientation and composition between grains lead to boundaries with different structure and mechanical relaxation times. A spectrum of activation energies can be expected for polycrystalline substances leading to broad internal-friction peaks. Few data are available for rocks, but a broad spread of activation energies is probable. This could lead to a Q roughly independent of frequency over a wide frequency band.

The effect on the grain-boundary peak caused by substitutional and impurity defects suggests that it is due to grain-boundary migration rather than sliding. Substitutional impurities increase the activation energy for the grain-boundary peak and reduce its height. Migration of atoms from one grain to another driven by the applied stress is identical to grain-boundary diffusion.

Grain-boundary damping is not really a separate phenomenon from those previously discussed but represents the increased effectiveness of these mechanisms in the boundary regions. The most plausible explanation of grain-boundary damping is essentially the same as stress-induced migration of atoms or reordering of the atoms and atomic bonds in and across the boundary. Partial melting is a variant of grain-boundary attenuation (Nur, 1971; Mavko and Nur, 1975).

High-temperature Thermally Activated Internal Friction and Transient Creep

At high temperatures, attenuation increases rapidly with temperature:

$$Q^{-1} = Q_0^{-1} e^{-E^*/RT}$$

This high-temperature background generally dominates at one-half the melting temperature and above. It increases exponentially with temperature and is a function of frequency and grain size but is independent of amplitude, at least to strains less than about 10^{-5} . The general functional form is

$$\begin{aligned} Q^{-1}(\omega) &= Q_0^{-1}(\omega\tau)^{-\alpha} \\ &= Q_0^{-1}(\omega\tau_0)^{-\alpha} \exp(-\alpha E^*/RT) \end{aligned} \quad (13)$$

where Q_0^{-1} and α are constants, E^* is an apparent activation energy and τ is a characteristic time. α is generally between $1/4$ and $1/2$. When E^* is known from diffusion or creep experiments, the parameter α can be determined from the temperature dependence of Q^{-1} as well as from its frequency dependence.

Attenuation is closely related to transient creep; specifically, equation 13 implies a transient creep response of the form

$$\begin{aligned} \varepsilon(t) &= \varepsilon_0(t/\tau)^\alpha \\ &= \varepsilon_0(t/\tau_0)^\alpha \exp(-\alpha E^*/RT) \end{aligned} \quad (14)$$

where t is the time. This is in addition to the instantaneous elastic response. The transient response is appropriate for short-term and small-strain situations such as seismic-wave attenuation, tidal friction, damping of the Chandler wobble and postearthquake rebound. Note that the apparent activation energy, αE^* , is less than the true activation energy.

Many materials satisfy the transient creep law (equation 14) with α between $1/3$ and $1/2$. Such values are obtained for example from transient creep experiments on rocks at high temperature. Equations 13 and 14 are essentially equivalent: If attenuation is known as a function of frequency, transient creep can be determined and vice versa. Such equivalence can be applied fruitfully to the study and interpretation of seismic-wave attenuation and creep in the Earth.

When $\alpha = 1/3$, equation 14 is the well-known Andrade creep equation. This equation cannot hold for all time since it predicts infinite creep rate at $t = 0$ and a continuously decreasing strain rate as time increases. Real materials at high temperature with a constantly applied stress reach a steady-state creep rate at long time. As Jeffreys (1958) has pointed out, thermal convection is precluded for a material having the rheology of equation 14, and he has used this to argue against continental drift. This prohibition, however, only applies to relatively short times before steady state is established. For very small stresses the strain rate does approach zero at long times for some transient creep mechanisms, such as dislocation bowing under stresses less than those required for dislocation multiplication. The critical stress is $\sigma = Gb/l$ where G is the shear modulus, b is the Burger's vector and l is the dislocation length. For dislocation lengths greater than 10^{-3} cm, multiplication, and therefore steady-state creep, will occur for stresses as low as 10 bar.

Equations 13 and 14 are usually considered as merely phenomenological descriptions of the behavior of solids at high temperatures. However, they can be constructed from a linear superposition of elastic and viscous elements and are thus a generalization of the standard linear solid or the standard anelastic solid.

The creep response of the standard linear solid with a single characteristic relaxation time (actually the strain retardation time), τ , is

$$\varepsilon(t) = \sigma[J_u + \delta J(1 - \exp(-t/\tau))]$$

where σ is the stress, J_u the unrelaxed compliance (the reciprocal of the conventional high-frequency elastic modulus), and δJ is the difference between the relaxed (long-time or low-frequency) and unrelaxed (short-time or high-frequency) compliances.

A more general model involves a spectrum of retardation times. For a distribution or spectrum of characteristic times, $D(\tau)$, the creep is

$$\varepsilon(t) = \sigma \left[J_u + \delta J \int_0^\infty D(\tau) [1 - \exp(-t/\tau)] d\tau \right] \quad (15)$$

(Minster and Anderson, 1981). For a single characteristic time $D(\tau)$ is a delta function. The retardation spectrum should yield physically realizable creep behavior, particularly at short and long times. $D(\tau)$ will be assumed to be limited to a finite band (τ_1, τ_2) —the cutoffs are determined by the physics of the problem and depend on physical variables (such as diffusivity), geometric variables (such as diffusion paths), as well as the thermodynamic conditions.

The distribution function

$$D(\tau) = \begin{cases} \frac{\alpha}{\tau_2^\alpha - \tau_1^\alpha} \frac{1}{\tau^{1-\alpha}} & \text{for } \tau_1 \leq \tau \leq \tau_2 \\ 0 & \text{otherwise} \end{cases} \quad (16)$$

yields a creep response which can be approximated by

$$\varepsilon(t) \approx \sigma J_u \left[1 + \frac{\delta J}{J_u} \Gamma(1 - \alpha) \left(\frac{t}{\tau_2} \right)^\alpha \right], \quad (17)$$

$$\tau_1 \ll \tau \ll \tau_2$$

(Anderson and Minster, 1979). Comparison with equation 14 yields

$$\varepsilon_0 = \frac{\delta J}{J_u} \Gamma(1 - \alpha) = \frac{\delta M}{M_r} \Gamma(1 - \alpha) \quad (18)$$

where M_r refers to the relaxed modulus. Note that the characteristic time appearing in equation 14 is actually the upper cutoff τ_2 .

Furthermore, this model yields a finite initial creep rate

$$\dot{\varepsilon} = \sigma \delta J \frac{\alpha}{1 - \alpha} \frac{\tau_1^{\alpha-1} - \tau_2^{\alpha-1}}{\tau_2^\alpha - \tau_1^\alpha} \quad (19)$$

A finite creep rate at the origin was achieved differently by Jeffreys (1965), who proposed what he called the modified Lomnitz law:

$$\varepsilon(t) = \frac{\sigma}{M_u} \left[1 + \frac{q}{\alpha} \left\{ \left(1 + \frac{t}{\tau} \right)^\alpha - 1 \right\} \right] \quad (20)$$

so that

$$\varepsilon(t) = \frac{\sigma}{M_u} \left[1 + \frac{q}{\alpha} \left(\frac{t}{\tau} \right)^\alpha \right] \quad \text{for } t \gg \tau \quad (21)$$

By identification with equation 17 and 19 we obtain the correspondence

$$\tau = [\Gamma(2 - \alpha)]^{1/(1-\alpha)} \tau_1$$

$$q = [\Gamma(2 - \alpha)]^{1/(1-\alpha)} \frac{\delta J}{J_u} \left(\frac{\alpha}{1 - \alpha} \right) \left(\frac{\tau_1}{\tau_2} \right)^\alpha \quad (22)$$

Note that the time constant in Jeffreys' equation is related to the shortest relaxation time in the spectrum, τ_1 , which is less than 1 s for many materials at high temperature. The parameter q is related to the ratio τ_1/τ_2 , which can be very small. For a dislocation bowing mechanism τ is proportional to the dislocation length squared. A spread of two orders of magnitude in dislocation lengths gives τ_1/τ_2 equal to 10^{-4} .

The Q corresponding to equation 17 for frequencies, ω , such that

$$\omega \tau_1 \ll 1 \ll \omega \tau_2$$

is given by

$$Q(\omega) = \cot \frac{\alpha \pi}{2} + \frac{2J_u}{\pi \alpha \delta J} [(\omega \tau_2)^\alpha - (\omega \tau_1)^\alpha] \cos \frac{\alpha \pi}{2}$$

$$\approx \frac{2J_u}{\pi \alpha \delta J} (\omega \tau_2)^\alpha \cos \frac{\alpha \pi}{2} \quad (23)$$

since $\tau_2 \gg \tau_1$ and $\cot \alpha \pi / 2$ is small. Thus, by comparison with equation 13,

$$Q_0 = \frac{2J_u}{\pi \alpha \delta J} \cos \frac{\alpha \pi}{2} \quad (24)$$

Therefore Q is predicted to increase with frequency as ω^α . Geophysical data give α in the range of 0.15 to 0.5 for periods greater than about 1 s.

For high frequencies $1 \ll \omega \tau_1 \ll \omega \tau_2$,

$$Q(\omega) = (1 - \alpha) (J_u / \alpha \delta J) (\tau_2 / \tau_1)^\alpha (\omega \tau_1) \quad (25a)$$

At low frequencies,

$$Q(\omega) = (1 + \alpha) (J_r / \alpha \delta J) (\omega \tau_2)^{-1} \quad (25b)$$

For thermally activated processes the characteristic times depend on temperature:

$$\tau = \tau_0 \exp(E^*/RT)$$

Inserting this into equations 17 and 23 yields the experimental equations. It is clear that at very low temperature the characteristic times are long and Q is low. At very high temperatures Q is predicted to increase as ω^{-1} . Equations

tion 23 holds for intermediate temperatures and intermediate frequencies.

Regardless of its origin the high-temperature background damping seems to dominate other mechanisms when measurements are performed at sufficiently high temperature. Therefore, it is particularly important in geophysical discussions.

PARTIAL MELTING

Several seismic studies have indicated that increased absorption, particularly of S-waves, occurs below volcanic zones and is therefore presumably related to partial melting. Regional variations in seismic absorption are a powerful tool in mapping the thermal state of the crust and upper mantle. Preliminary results indicate that, where the absorption is anomalously high, V_s is more affected than V_p . It has also been suggested that partial melting is the most probable cause of the low-velocity layer in the upper mantle of the Earth (Anderson and Sammis, 1970). Thus the role of partial melting in the attenuation of seismic waves may be a critical one, at least in certain regions of the Earth.

Studies of the melting of polycrystalline solids have shown that melting begins at grain boundaries, often at temperatures far below the melting point of the main constituents of the grains. This effect is caused by impurities that have collected at the grain boundaries during the initial solidification. Walsh (1969) computed the internal friction for phenomenological models of a partially melted solid. His calculations included mechanical effects only, ignoring thermoelastic and thermochemical attenuation in two-phase systems.

Attenuation according to Walsh's model should exhibit the following properties:

1. Q_K^{-1} , the attenuation of the purely compressional component of seismic waves due to this mechanism, will be negligible at seismic frequencies.
2. Under shear, this material exhibits the properties of the standard linear solid with relaxation time roughly given by

$$1/\tau = a\mu/\eta$$

where μ is grain rigidity and η is melt viscosity. The ratio μ/η typically ranges from 10^4 to 10^8 Hz, so that this mechanism would be important for inclusion aspect ratios a , of 10^{-8} to 10^{-4} . These aspect ratios would be reasonable for a melt phase that wets the grain boundary, thus forming a thin film. Furthermore, the relaxation strength is strongly dependent on the number of sites of melting, and could exceed 1 even for a very small volume of melt.

3. This shear attenuation mechanism will behave as a thermally activated relaxation.

4. Shear attenuation will increase very sharply with the onset of melting.

The concentration of melt as a function of temperature and pressure is perhaps the most important unknown quantity, followed closely by the viscosity of the melt. As some partial melting is likely to occur in the Earth's mantle, this mechanism is a possible cause of seismic attenuation, particularly at very low frequencies. Melt concentrations of as little as 10^{-2} may cause significant attenuation at seismic frequencies.

Spetzler and Anderson (1968) studied the effect of partial melting in the system NaCl-H₂O. At the eutectic temperature the system is partially molten, having a melt content that is proportional to the original salinity. The internal friction for longitudinal waves increased abruptly by 48 percent at the eutectic point for 1 percent partial melting and 71 percent for 2 percent partial melting. The corresponding increases in internal friction for shear were 37 percent and 73 percent. Further melting caused a gradual further increase in Q^{-1} . The fractional increases in Q^{-1} across the eutectic point were much greater than the fractional drops in velocity. Figure 14-4 shows the Q in the ice-brine-NaCl system for a concentration of 2 percent NaCl for longitudinal vibrations of a rod. Plotted are data for the fundamental and first two overtones. Note the abrupt drop in Q as partial melting is initiated at the eutectic temperature. There is a corresponding, but much less pronounced, drop in velocity at the same temperature.

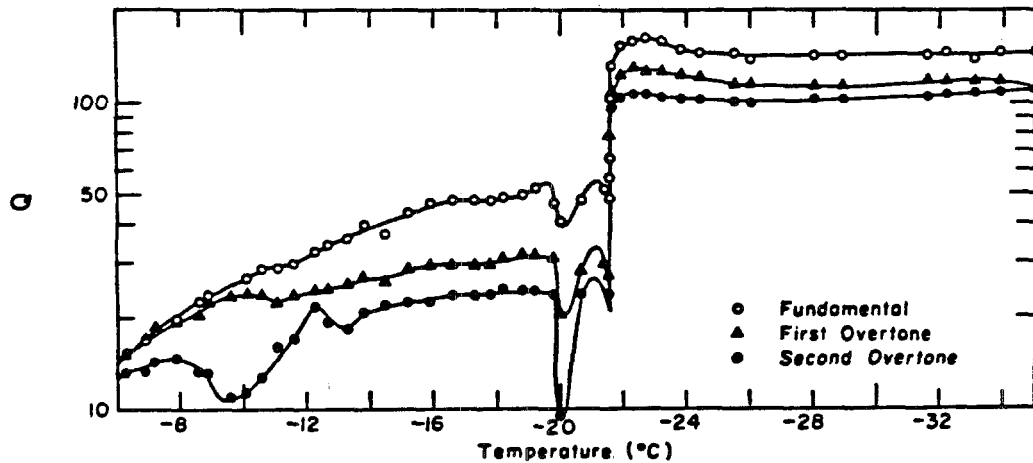
BULK ATTENUATION

Most of the mechanisms of seismic-wave attenuation operate in shear. Shear losses, generally, are much larger than compressional losses, and therefore shear waves attenuate more rapidly than compressional waves. Bulk or volume attenuation can become important in certain circumstances. One class of such mechanisms is due to thermoelastic relaxation. An applied stress changes the temperature of a sample relative to its surrounding, or of one part of a specimen relative to another. The heat flow that then occurs in order to equalize the temperature difference gives rise to energy dissipation and to anelastic behavior. The change in temperature is simply

$$(\partial T/\partial P)_s = -\alpha T/C_p$$

and the difference between the unrelaxed and relaxed moduli is the difference between the adiabatic and isothermal moduli. Under laboratory conditions this is typically 1 percent for oxides and silicates. α is the coefficient of thermal expansion.

In a propagating longitudinal wave the regions of compression (hot) and dilatation (cold) are separated by a half-wavelength, $\lambda/2$, where $A = c/f$. The relaxation time is


FIGURE 14-4

Q of ice containing 2 percent NaCl. At low temperatures this is a solid solution. At temperatures higher than the eutectic the system is an ice-brine mixture (Spetzler and Anderson, 1968).

$$\tau = \lambda^2 / (2\pi)^2 \kappa$$

where κ is the thermal diffusivity. Attenuation is maximum at

$$\omega\tau = c\lambda / 2\pi\kappa$$

Peak damping occurs at very high frequencies ($>10^{10}$ Hz), and this mechanism is therefore unimportant at seismic frequencies and most ultrasonic experiments. The hot and cold parts of the wave are too far apart for appreciable heat to flow during a cycle. On the other hand experiments in the gigahertz range, as in Brillouin scattering, may actually be measuring the isothermal rather than the adiabatic moduli. This may be counterintuitive since static, or long-term, deformation experiments also give the isothermal moduli. The explanation is that heat flow depends both on the time scale and the length scale. Although only a short time is available in the high-frequency experiments, the length scale, or wavelength, is also very short.

A variant of this mechanism has to do with intergranular thermal currents. In a polycrystalline material another length scale is determined by the grain size. When a stress is applied to an inhomogeneous or polycrystalline material, different parts are compressed differently and intergranular thermal currents are set up. The magnitude of the effect depends on the anisotropy and heterogeneity of the grains. The characteristic relaxation time is now in proportion to d^2/κ where d is the grain size, and Q is a unique function of fd^2/κ . The theory for this mechanism (Zener, 1948) shows that the absorption peak is broader than a Debye peak on the high-frequency side, and Q increases as $\omega^{1/2}$, rather than as ω for a Debye peak appropriate for the standard linear solid. At low frequencies $Q \approx \omega^{-1}$, as for a Debye peak. The relaxation time is

$$\tau = d^2 / 3\pi^2 \kappa$$

In polycrystal materials the flow of heat may take place between adjacent grains because of differential compression. This can occur even in solids where the grains are of identical composition if they are anisotropic and un-oriented. This latter situation gives

$$Q^{-1} = \left(\frac{C_P - C_V}{C_V} \right) R \frac{\omega\omega_0}{\omega^2 + \omega_0^2}$$

where the first term on the right is the relative difference between the specific heats, R is a factor that increases with the anisotropy of the grains and ω_0 is the intergranular relaxation frequency. Again the damping is a maximum when $\omega_0\tau \approx 1$ or approximately

$$\omega^{-1} = \tau \approx 10^3 d^2$$

For very anisotropic crystals this mechanism gives $Q \approx 10^3$ at maximum damping. The grain size in the upper mantle is uncertain, but for $d = 1$ mm to 1 m the critical wave period for maximum attenuation is 10^{-1} to 10^7 s. The range of grain sizes and thermal properties in a common rock would tend to broaden the relaxation peak. In the nearly adiabatic high-frequency case, the thermal currents are confined to the immediate vicinity of the grain boundaries and the internal friction varies as $\omega^{-1/2}$; this for wavelengths short compared to the grain dimensions. An approximate calculation gives

$$Q^{-1} \approx \Delta\Omega(\mathcal{K}/C_V)(2\omega)^{-1/2}$$

where Ω is the ratio of total surface area to volume. In the other extreme, isothermal vibrations (small grain sizes and low frequency), the internal friction is proportional to the first power of frequency. \mathcal{K} is thermal conductivity.

By appropriate choice of parameters, primarily the distribution of grain sizes, one can obtain a Q that is frequency independent over a broad spectrum. The internal friction, Q^{-1} , increases slightly faster than linearly with temperature for thermoelastic mechanisms. Except for the contribution of open cracks, which presumably dominates the damping at low pressure, the effect of pressure can be expected to be slight. Intergranular thermoelastic stresses are suppressed by pressure primarily to the extent that anisotropy and mechanical heterogeneity are reduced.

Thermoelastic losses are intimately related to changes in volume and, therefore, are usually more effective for compressional waves than for pure shear waves. However, when inhomogeneities are imbedded in a material, shear waves as well as compressional waves generate local dilatational stress inhomogeneities and, therefore, can have thermoelastic components in their damping. In fact, it is possible to contrive geometries that lead to greater shear wave attenuation than longitudinal wave attenuation.

Thermoelastic losses undoubtedly exist in materials as inhomogeneous as those thought to make up the mantle. Anisotropic grains with random orientation, the close association of grains with different elastic and thermal properties and the possible existence of molten regions all would tend to introduce local fluctuations in stress with an attendant thermal diffusion. The wide spectrum of grain sizes, anisotropies, orientations and physical properties of rock-forming minerals tend to smear out the thermoelastic peak and broaden the Q spectrum over a wide frequency band.

Table 14-2 shows the peak frequency expected for a range of possible grain sizes, using the properties of forsterite. The maximum internal friction will occur in the range of seismic frequencies if the grain size in the mantle is in the range of 1 to 100 cm. The magnitude of the peak internal friction is harder to estimate. Most experiments have been performed on cubic metals with isotropic coefficients of thermal expansion, so that the anisotropy factor R has reflected only the elastic anisotropy. In rocks, particularly multicomponent rocks, anisotropy of thermal expansion will be significant, and the elastic anisotropy will probably exceed that of metals. The effect of variations in grain size in rocks would be to weaken the frequency dependence of the internal friction. Taking these effects into account, it is estimated that the internal friction from this mechanism, could reach 10^{-3} to 10^{-2} in the mantle. For shear waves, the attenuation would probably be somewhat less but could still be significant. Substantial shear strains can be introduced in a heterogeneous solid by a purely longitudinal applied stress.

The peak attenuation depends on the contrast, amongst the grains, in bulk modulus and thermal expansion. If a composite contains grains that are very anisotropic or differ greatly in their properties, the bulk attenuation can be substantial. For a factor of 2 contrast in the coefficient of thermal expansion or bulk modulus, Q_K can be as low as

300 and 3000, respectively (Budiansky and O'Connell, 1980). Bulk attenuation of this type depends on the differences in the properties of the constituent grains and is therefore a possibly useful constraint on the petrology of the mantle.

In an application of the theory, Budiansky and O'Connell (1980) showed that a lower mantle composed of stishovite and magnesiowüstite and having grain sizes in the range 3 mm to 1 m can be ruled out on the basis of the maximum Q_K allowed by the damping of the radial mode ${}_0S_0$. Q_K , for this mechanism, is not a thermally activated process and therefore is only a weak function of temperature and pressure. A change in mineralogy, however, associated with a change in pressure or temperature, or a change in grain size and orientation, due to a change in stress, can affect Q_K . The peak frequency is related to the grain size.

There is another effect associated with polycrystalline material. A volumetric strain produces local shear deformations within the individual grains (Heinz and others, 1982). This leads to Q_K^{-1} of the order of 1 percent of Q_G^{-1} , and the variation of Q_K with temperature and frequency will follow the variation of Q_G . Q_K is difficult to measure in the Earth since it is generally higher than the Q_G , which therefore dominates the attenuation of seismic energy over most frequency bands.

The radial modes (${}_0S_0$, ${}_1S_0$, ${}_2S_0$, etc.) are affected by Q_K and are less sensitive to Q_G . In fact, these modes are observed to have very high Q . Unfortunately, they have little resolving power, and it is not even clear if it is the mantle or the core that is responsible. In regions of the mantle or the spectrum where Q is large, it may be possible to study Q_K from the attenuation of compressional waves.

RELAXATIONS IN SYSTEMS UNDERGOING PHASE TRANSFORMATIONS

In systems subject to solid-liquid or solid-solid phase transitions, small stresses can induce a reaction from one phase to another, causing stress relaxation and bulk attenuation. For two phases in equilibrium, the attenuation is given by the standard relaxation formula

$$Q^{-1} = \Delta \frac{\omega\tau}{1 + (\omega\tau)^2}$$

Δ is evaluated from the thermodynamic properties of the system by using

$$K_i = (\partial P / \partial \rho)_i = \left(\frac{-\gamma V}{\rho(\partial V / \partial P)_T} \right)_i$$

where V is the molar volume, K_i is the bulk modulus and γ is the ratio of specific heats:

TABLE 14-2
Frequency Dependence of Thermoelastic Attenuation as a Function of Grain Size in Forsterite

Grain Size (cm)	Peak Frequency (Hz)
10^{-2}	10^3
10^{-1}	10
1	10^{-1}
10	10^{-2}
10^2	10^{-5}

$$\gamma_i = (C_p/C_v) = \left[\frac{C_p}{C_p + T(\partial V/\partial T)_P^2/(\partial V/\partial P)_T} \right]_i$$

This theory holds when both phases are present and in equilibrium. At the temperature of onset of a phase change, discontinuous volume changes occur that require a modified analysis. For most solid-liquid transitions, and for solid-solid transitions of geophysical interest, the relaxation strength will be large, of the order of magnitude 10^{-1} to 1. The peak frequency is determined by the kinetics of the appropriate reaction.

The subscript *i* refers to *u* (unrelaxed or infinite frequency) or *r* (relaxed or zero frequency). At infinite frequency K_u is simply a volume average of the bulk moduli of the components, at constant extent of reaction. That is, the amount of each phase does not change with temperature or pressure. K_r includes the normal elastic deformation plus the volume change due to reaction. This gives a smaller effective modulus.

The Vaisnys (1968) theory treats the attenuation of acoustic waves propagating through a system undergoing phase transition where a finite reaction rate introduces a lag between the applied pressure change and the response. Stevenson (1983) treated the case of infinite reaction rate but a diffusive lag of heat and matter across the phase boundary. Irreversible entropy production accompanies the imposition of a pressure or temperature perturbation on a two-phase system consisting of a dilute suspension of a solid phase in a liquid. The minimum *Q* in this case occurs at a frequency

$$\omega_0 = 4\pi D/l\phi$$

where *D* is the solute diffusivity, *l* is the dimension of the solid particles and ϕ is volume concentration of particles. $Q \approx \omega^{1/2}$ in the high frequency limit, as appropriate for a diffusive mechanism, and $Q \approx \omega$ in the low-frequency limit, in common with other mechanisms. For well separated particles there is also a $Q \approx \omega^{-1}$ regime. This mechanism might be important in magma chambers and in subliquidus parts of the core. In principle, it also applies for solid-solid phase changes but requires small grain sizes, high diffusivities and low-frequency waves.

PHYSICS OF ATTENUATION IN FLUIDS

The absorption of sound in a liquid at low frequencies is given by

$$k^*/f^2 = (2\pi^2/\rho c^3) \left\{ \frac{4}{3} \eta_s + (c^2 \alpha^2 \mathcal{K}/C_p) + \eta_v \right\}$$

where k^* is the spatial attenuation coefficient, α is the coefficient of thermal expansion, \mathcal{K} the thermal conductivity, η_s the shear viscosity, η_v the volume viscosity and *f* is frequency. The first two terms on the right-hand side represent the classical Stokes-Kirchoff absorption due to shear stresses and thermal conductivity. The first term is important in the attenuation of longitudinal waves in liquid metals but is absent for strains involving pure compression. The second term is important in liquid metals at laboratory frequencies, but is negligible at core conditions and seismic frequencies. The remaining term is called the excess absorption and is due to bulk or volume viscosity. In liquid metals at low pressure, η_v is similar in magnitude to η_s .

Several mechanisms contribute to bulk viscosity in simple fluids. One is structural relaxation due to perturbations in the short-range order caused by the sound wave. Another is due to concentration fluctuations in alloy systems. The characteristic times for shear and structural relaxation are likely to be similar as they are both controlled by short-range diffusion. The relaxation time due to concentration fluctuations or chemical reactions may be quite different.

Longitudinal waves in liquid metals typically are within an order of magnitude of

$$Q = 10^{11}/f$$

which, under normal conditions is composed of roughly equal parts contributed by shear viscosity, thermal conductivity and bulk viscosity. The attenuation in liquid metals at seismic frequencies would be quite negligible. However, the effects of pressure and alloying lengthen the characteristic relaxation times.

The bulk viscosity of a pure liquid metal is due to structural rearrangement as there are no internal degrees of freedom. Two-state theories have been developed to explain structural relaxation associated with pressure changes. The assumption is that a liquid is a mixture of two structural states with differing mole volumes and energies.

The two-state theory (Flinn and others, 1974) can be used to estimate the structural volume viscosity of iron just above the melting point, T_m , and its relation to the shear viscosity:

$$\eta_v = \frac{x_1 x_2 V}{RT_m} \left(\frac{\Delta V}{V} - \frac{\alpha \Delta H}{C_p} \right)^2 \tau K^2$$

and

$$\eta_v/\eta_s = \frac{(2n-12)(12-n)}{n^2} \left(\frac{VK}{RT_m} \right)^2 \left(\frac{\Delta V}{V} - \frac{\alpha \Delta H}{C_p} \right)^2$$

$$x_2 = (12-n)/n = 1 - x_1$$

where x_1 and x_2 are the mole fractions of the two states, which differ by ΔV and ΔH in molar volume and enthalpy, and n is the coordination number. For liquid iron at low pressure we take $n = 9$; $V = 8 \text{ cm}^3/\text{mol}$; $\Delta V/V = 0.1$; $\Delta H/RT_m = 3$; the bulk modulus $K = 1.3 \text{ Mbar}$ (10 percent less than solid iron); $\alpha = 70 \times 10^{-6}/\text{K}$, $C_p = 10.2 \text{ cal/mol K}$; and the relaxation time, $\tau = 5 \times 10^{-12} \text{ s}$. This relaxation time is typical of liquid metals. These parameters give

$$\eta_v = 3 \times 10^{-2} \text{ poise} = 3 \text{ cP}$$

and

$$\eta_s = (5/3)\eta_v = 5 \text{ cP}$$

for molten iron at low pressure. The measured value for η_s is 4.8–7.0 cP, and the near equality of η_s and η_v is consistent with measurements on other liquid metals. Thus, the two-state theory gives satisfactory results at low pressure, which leads us to investigate the properties at core conditions.

The main effect of pressure and temperature is on the bulk modulus K and the relaxation time τ . The bulk modulus of the core is 4–10 times larger than iron at normal conditions, and relaxation times have been estimated to be of the order of 10^{-8} – 10^{-9} s . Therefore, bulk viscosities four to six orders of magnitude larger than at low pressures, or η_v of 10^2 – 10^4 P , are expected. The associated shear viscosities would be in the range of 10–100 P. The neglect of the effect of temperature and pressure on the other parameters would decrease these estimates slightly but probably by less than an order of magnitude. An upper limit for η_s at the top of the outer core is 10^6 P based on the lack of damping of the 18.6-year principal nutation (Toomre, 1974). A strong magnetic field in the core can result in a magnetic viscosity that is in addition to these structural relaxations. The magnetic viscosity is anisotropic, controlled by the orientation of the magnetic field. Seismic waves traveling in a core with a magnetic field of the order of 10^5 gauss would have a measurable anisotropy. Slow shear waves would also propagate in the "liquid" core.

Effect of Alloying

Based on density and cosmic abundances, the core is likely to contain up to 10 percent nickel and other siderophiles and a similar amount of a light element such as oxygen or sulfur. There are additional volume relaxation mechanisms associated with alloys and solutions. In particular the relaxation times can be much longer than those due to shear and structural relaxations. This might be significant in explaining the apparent frequency dependence of Q of P-waves in

the outer core. There is a suggestion of a linear increase of Q_p with frequency, which, if verified, indicates that the seismic band is on the high-frequency side of the absorption band in the outer core (Anderson and Given, 1982). As this cannot be true for shear waves unless the unrelaxed shear modulus of the core is much lower than the rigidity of the inner core, we may need a low-frequency volume relaxation mechanism. This contribution to the bulk attenuation and volume viscosity depends on concentration and may eventually shed light on the nature of alloying elements in the core.

Flinn and others (1974) found a highly temperature-dependent absorption mechanism operating in binary melts that is not present in the pure metals. The extra absorption in liquid metal alloys is probably due to concentration fluctuations. Theoretically, it is inversely proportional to the diffusivity or directly proportional to the shear viscosity. As with the structural viscosity, it is also proportional to the square of the bulk modulus and can therefore be expected to increase with pressure. More importantly, it is a function of the curvature of the Gibbs potential versus concentration relation and, therefore, becomes very large in the vicinity of a critical point. Unfortunately, it is not possible to estimate the relaxation time of this mechanism in the core.

We can conclude that structural and concentration fluctuations may be responsible for bulk viscosity in the core and contribute to the excess absorption of the radial modes.

Relaxation Theory of Bulk Attenuation in the Core

The Q due to bulk losses in a relaxing solid or viscoelastic fluid is

$$Q_K^{-1}(\omega) = (\Delta K/K)\omega\tau_v/(1 + \omega^2\tau_v^2) \quad (26)$$

where $\Delta K/K = A$ is the modulus defect and τ_v is the volume relaxation time. The modulus defect is the fractional difference between the high-frequency and low-frequency moduli. This has not been measured for liquid metals but is typically about 0.3 for other liquids. The decrease in bulk modulus on melting of metals ranges from about 5 to 30 percent. This may be of the same order as the modulus defect for molten metals. The bulk moduli of glasses are often taken as approximately the same as the high-frequency moduli for fluids. This gives a modulus defect of 0.2–0.7 for most liquid-glass systems. These estimates give Q_{\min} between 10 and ≈ 3 at $\omega\tau = 1$. The increase in bulk modulus at the inner core–outer core boundary is about 5 percent. If this is taken as $\Delta K/K$, we obtain an estimate of 40 for the minimum Q_K of the core at $\omega\tau = 1$. A Q_K of 2×10^3 at a period of 20 min (the period of ${}_0S_0$) implies, equation (26), that $\tau \approx 4 \text{ s}$ or 10^4 s . The smaller value would be consistent with the solid-like behavior of the inner core for short-period body waves. The location of the inner core–outer

core boundary would then be frequency dependent, and the inner core would apparently be smaller at free-oscillation periods. Such a frequency dependence has, in fact, been suggested by Gutenberg (1957). A frequency-dependent inner-core boundary could explain the discrepancy between the free-oscillation and body-wave determinations of the properties of the inner core. For example, the shear velocity obtained for the inner core from short-period waves is about 20 percent smaller than that obtained from the free-oscillation data for a fixed inner core radius. These results can equally well be interpreted in terms of a 20 percent decrease in inner-core radius in going from body-wave to free-oscillation periods. Glass-like transitions, or transitions from fluid-like to solid-like behavior, typically take place over a small range of temperature. The sharpness of the inner-core boundary could be explained by such a transition occurring over a small range of pressure.

Interpreting the data in this way requires that the seismic data for the outer core be on the low-frequency side of the relaxation peak (Anderson, 1980). For the outer core,

$$Q_{\bar{\kappa}}^{-1} = \frac{\Delta K}{K} (\omega\tau_v)$$

and for the inner core,

$$Q_{\bar{\kappa}}^{-1} = (\Delta K/K)/\omega\tau_v$$

The boundary of the inner core, then, corresponds to $\omega\tau = 1$, and this is where attenuation would be a maximum. For a 1-s body wave the inferred relaxation time at the inner core–outer core boundary is $(2\pi f)^{-1}$ or about 0.2 s. This is close to the value deduced from $Q_{\bar{\kappa}}$ in the outer core.

ABSORPTION-BAND Q MODEL FOR THE EARTH

Attenuation in solids and liquids, as measured by the quality factor Q , is typically frequency dependent. In seismology, however, Q is usually assumed to be independent of frequency. The success of this assumption is a reflection of the limited precision, resolving power and bandwidth of seismic data and the trade-off between frequency and depth effects rather than a statement about the physics of the Earth's interior.

Frequency-independent Q models provide an adequate fit to most seismic data including the normal-mode data (Anderson and Archambeau, 1964; Anderson and others, 1965; Anderson and Hart, 1979). There is increasing evidence, however, that short-period body waves may require higher Q values. Some geophysical applications require estimates of the elastic properties of the Earth outside the seismic band. These include calculations of tidal Love numbers, Chandler periods and high-frequency moduli for com-

parison with ultrasonic data. The constant- Q models cannot be used for these purposes. For these reasons it is important to have a physically sound attenuation model for the Earth.

The theory of seismic attenuation has now been worked out in some detail (Anderson and Minster, 1979; Minster and Anderson, 1981). Although a mild frequency dependence of Q can be expected over a limited frequency band, Q or Q^{-1} should be a linear function of frequency at higher and lower frequencies.

For a solid characterized by a single relaxation time τ , Q^{-1} is a Debye function with maximum absorption at $\omega\tau = 1$. For a solid with a spectrum of relaxation times, the band is broadened and the maximum attenuation is reduced. For a polycrystalline solid with a variety of grain sizes, orientations and activation energies, the absorption band can be appreciably more than several decades wide. If, as seems likely, the attenuation mechanism in the mantle is an activated process, the relaxation times should be a strong function of temperature and pressure. The location of the absorption band, therefore, changes with depth. The theory of attenuation in fluids indicates that Q in the outer core should also depend on frequency.

The theoretical considerations in this chapter indicate that Q can be a weak function of frequency only over a limited bandwidth. If the material has a finite elastic modulus at high frequency and a nonzero modulus at low frequency, there must be high- and low-frequency cutoffs in the relaxation spectrum. Physically this means that relaxation times cannot take on arbitrarily high and low values. The relationship between Q and bandwidth indicates that a finite Q requires a finite bandwidth of relaxation times and therefore an absorption band of finite width. Q can be a weak function of frequency only in this band.

We can approximate the absorption band in the following way:

$$Q = Q_m (f\tau_2)^{-1}, \quad f < 1/\tau_2$$

$$Q = Q_m (f\tau_2)^a, \quad 1/\tau_2 < f < 1/\tau_1$$

$$Q = Q_m (\tau_2/\tau_1)^a (f\tau_1), \quad f > 1/\tau_1$$

where $f (= \omega/2\pi)$ is the frequency, τ_1 is the short-period cutoff, τ_2 is the long-period cutoff and Q_m is the minimum Q , which occurs at $f = 1/\tau_2$ if $a > 0$. These parameters are shown in Figure 14-5. This approximation of an absorption band was used by Anderson and Given (1982) to model the attenuation in the mantle and core.

The relaxation time, τ , for an activated process depends exponentially on temperature and pressure. The characteristic time τ_0 depends on l^2 and D for diffusion-controlled mechanisms where l and D are characteristic length and a diffusivity, respectively. Characteristic lengths, such as dislocation or grain size, are a function of tectonic stress, which is a function of depth. The location of the band, therefore, depends on tectonic stress, temperature and pressure. The width of the band is controlled by the

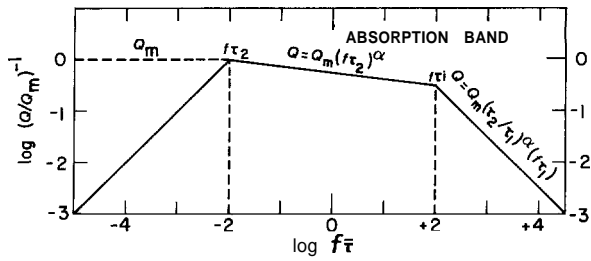


FIGURE 14-5 Schematic illustration of an absorption band (Anderson and Given, 1982).

distribution of relaxation times, which in turn depends on the distribution of grain sizes or dislocation lengths.

With an activation energy of 60 kcal/mole, τ decreases by about an order of magnitude for a temperature rise of 200°C. An activation volume of 10 cm³/mole causes τ to increase by an order of magnitude for a 30-kbar increase in pressure. In regions of low temperature gradient, the maximum absorption shifts to longer periods with increasing depth. This condition is probably satisfied throughout most of the mantle except in thermal boundary layers. Characteristic lengths such as grain size and dislocation length decrease with increasing stress. A decrease in tectonic stress by a factor of 3 increases the relaxation time by about an order of magnitude. A decrease of stress with depth moves the absorption band to longer periods.

The effect of pressure dominates over temperature for most of the upper mantle, and tectonic stress probably decreases with depth. Therefore the absorption band is expected to move to longer periods with increasing depth. A reversal of this trend may be caused by steep stress or temperature gradients across boundary layers, or by enhanced diffusion due to changes in crystal structure or in the nature of the point defects. For a given physical mechanism there are relationships between the width of the band (τ_2/τ_1), Q_m and α ; that is, these three parameters are not independent.

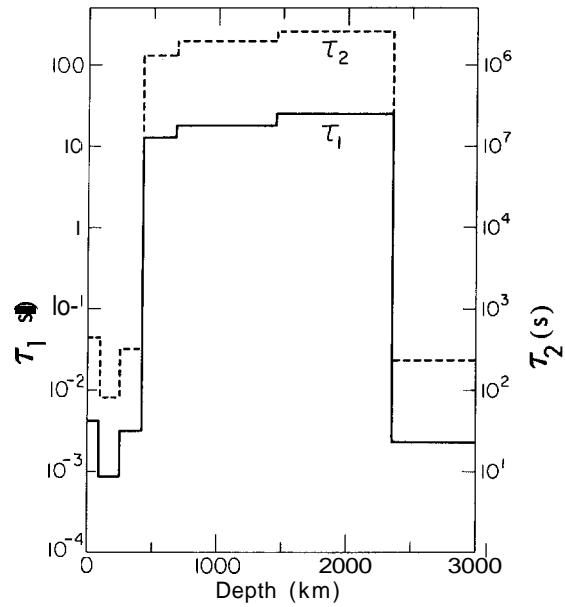


FIGURE 14-6 τ_1 and τ_2 as a function of depth in the mantle for the absorption-band model (ABM) for Q_s (Anderson and Given, 1982).

For fixed α , τ_2/τ_1 increases as Q_m^{-1} decreases. If we assume that the parameters of the absorption band, Q_m^{-1} , τ_1/τ_2 and α , are constant throughout the mantle, we can use the seismic data to determine the location of the band as a function of depth, or $\tau_1(z)$. This assumption is equivalent to assuming that the activation energy, E^* , and activation volume, V^* , are fixed. By assuming that the characteristics of the absorption band are invariant with depth, we are assuming that the width of the band is controlled by a distribution of characteristic relaxation times rather than a distribution of activation energies. Although this assumption can be defended, to some extent it has been introduced to reduce the number of model parameters. If a range of activation energies is assumed, the shape of the band (its width and height)

TABLE 14-3 Absorption Band Parameters for Q_s

Radius (km)	Depth (km)	τ_1 (s)	τ_2/τ_1	$Q_s(\text{min})$ (τ_1)	Q_s (100 s)	α
1230	5141	0.14	2.43	35	1000	0.15
3484	2887	—	—	—	—	—
4049	2322	0.0025	10^5	80	92	0.15
4832	1539	25.2	10^5	80	366	0.15
5700	671	12.6	10^5	80	353	0.15
5950	421	0.0031	10^5	80	330	0.15
6121	250	0.0009	10^5	80	95	0.15
6360	11	0.0044	10^5	80	90	0.15
6371	0	0	∞	500	500	0

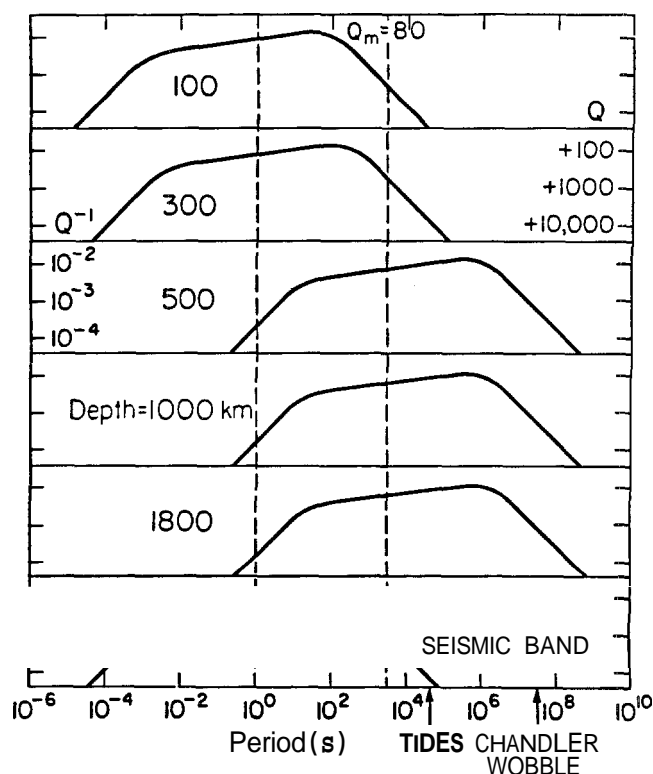


FIGURE 14-7
The location of the absorption band for Q_s as a function of depth in the mantle (Anderson and Given, 1982).

varies with temperature and pressure. The parameters of the absorption bands are given in Table 14-3. The locations of the bands as a function of depth are shown in Figures 14-6, 14-7 and 14-8. I will refer to the absorption-band model as ABM. The parameter a can be adjusted by trial and error: $a = 0.3$ is too high and $a = 0.15$ is about right.

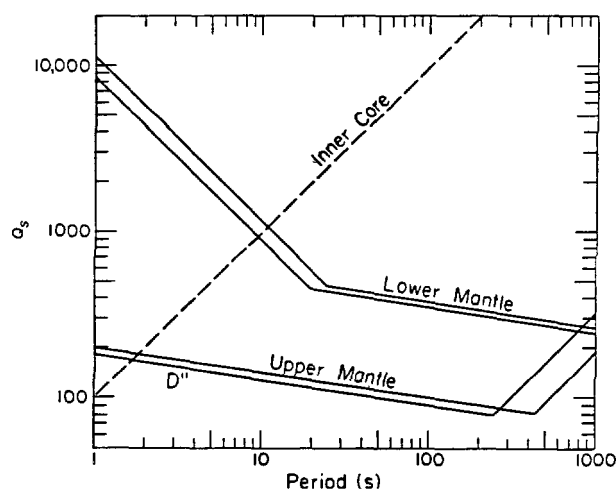


FIGURE 14-8
 Q_s as a function of period for the mantle and inner core for ABM. Note the similarity of the upper mantle and the lowermost mantle (D). These may be thermal (high-temperature gradient) and mechanical (high-stress) boundary layers associated with mantle convection (Anderson and Given, 1982).

The variation of τ_1 and τ_2 with depth in the mantle is shown in Figure 14-6. Note that both decrease with depth in the uppermost mantle. This is expected in regions of steep thermal gradient. They increase slightly below 250 km and abruptly at 400 km. No abrupt change in τ_1 or τ_2 occurs at 670 km. Apparently, a steep temperature gradient and high tectonic stresses can keep the absorption band at high frequencies throughout most of the upper mantle, but these effects are overridden below 400 km where most mantle minerals are in the cubic structure. A phase change, along with high pressure and low stress, may contribute to the lengthening of the relaxation times. Relaxation times change only slightly through most of the lower mantle.

TABLE 14-4
 Q_s and Q_p as Function of Depth and Period for Model ABM

Depth (km)	Q_s				Q_p			
	1s	10s	100s	1000s	1s	10s	100s	1000s
5142	100	1000	10,000	10^5	511	454	3322	3.3×10^4
4044	—	—	—	—	4518	493	1000	10^4
2887	—	—	—	—	7530	753	600	6000
2843	184	130	92	315	427	345	247	846
2400	184	130	92	315	427	345	247	846
2200	11,350	1135	366	259	2938	2687	942	668
671	8919	892	353	250	2921	2060	866	615
421	5691	569	330	234	741	840	819	603
421	190	134	95	254	302	296	244	659
200	157	111	90	900	270	256	237	2365
11	200	141	100	181	287	262	207	377
11	500	500	500	500	487	767	1168	1232

TABLE 14-5
Average Mantle Q Values as Function of Period, Model ABM

Region	0.1s	1s	4s	10s	100s	1000s
			Q_s			
Upper mantle	379	267	210	173	127	295
Lower mantle	1068	721	520	382	211	266
Whole mantle	691	477	360	280	176	274
			Q_p			
Upper mantle	513	362	315	354	311	727
Lower mantle	586	1228	1262	979	550	671
Whole mantle	562	713	662	639	446	687
		$Q({}_0S_2)$				
	3232 s		12 h		14 mos	
	596		514		463	

TABLE 14-6
Relaxation Times (τ_1, τ_2) and Q_K for Bulk Attenuation at Various Periods

Region	τ_1 (s)	τ_2 (s)	Q_K			
			1s	10s	100s	1000s
Upper mantle	0	3.33	479	1200	1.2×10^4	1.2×10^5
Lower mantle	0	0.20	2000	2×10^4	2×10^5	2×10^6
Outer core	15.1	66.7	7530	753	600	6000
	9.04	40.0	4518	493	1000	10,000
Inner core	3.01	13.3	1506	418	3000	3×10^4

Q_K (min) = 400, $\alpha = 0.15$.

The location of the absorption band is almost constant from a depth of about 400 to 2000 km (Figure 14-6). Most of the lower mantle therefore has high Q_s for body waves and low Q_s for free oscillations (Tables 14-4 and 14-5). The low-order spheroidal modes require a distinctly different location for the absorption band in the lower 500 km of the mantle. These data can be satisfied by moving the band to the location shown in the lower part of Figure 14-7. This gives a low-Q region at the base of the mantle at body-wave periods.

Under normal conditions, fluids in general and molten metals in particular satisfy the relaxation equations, with $\omega\tau \ll 1$ giving $Q \propto \omega^{-1}$. Pressure serves to increase mean relaxation time $\bar{\tau}$, and the high absorption of short-period P-waves in the inner core suggests that $\bar{\tau}$ may be of the order of 1 s in this region (Anderson, 1980). The high Q of the outer core at body-wave frequencies suggests that the absorption band is at longer or shorter periods.

If Q in the core is assumed to be a Debye peak, with fixed Q_p and width, we find that $Q_p = 400$ and $\bar{\tau}$ decreases with depth from 32 to 19 s in the outer core to 6 s in the inner core.

The net result is a slowly varying Q_p , 406 to 454, for the inner core between 0.1 and 10 s, increasing to 3320 at

100 s and 3.3×10^4 at 1000 s. Most studies of Q_p of the inner core at body-wave frequencies give values between 200 and 600 (Anderson and Archambeau, 1964). In the outer part of the outer core Q_p for ABM decreases from 7530 at 1 s to 753 at 10 s and then increases to 6000 at 1000 s. The relative location of the band is fixed by the observation that short-period P-waves see a high-Q outer core and a low-Q inner core. The absorption band model predicts relatively low Q for 10–50-s P-waves in the outer core. Data are sparse, but long-period P-waves in the outer core may be attenuated more than short-period waves (Anderson and others, 1965).

The attenuation of shear waves, Love and Rayleigh waves, toroidal oscillation and most of the spheroidal modes are controlled almost entirely by Q_s in the mantle. Once the mantle Q_s is determined, the Q of P-waves and the high-Q spheroidal and radial modes can be used to estimate Q_K , as shown in Figure 14-9 and listed in Table 14-6. The relationship between Q_p , Q_s and Q_K is

$$Q_p^{-1} = LQ_s^{-1} + (1 - L)Q_K^{-1}$$

where $L = (4/3)(\beta/\alpha)^2$ and β and α are the shear and compressional velocities. For a Poisson solid with $Q_K^{-1} = 0$,

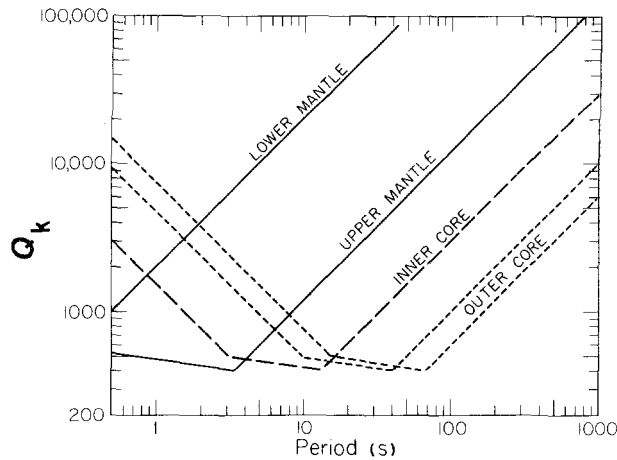


FIGURE 14-9
 Q_k as a function of frequency for various regions in the Earth (Anderson and Given, 1982).

$$Q_p = (9/4)Q_s$$

The ABM average Earth model was used as a starting model to satisfy a variety of seismic data for the Eurasian shield by Der and others (1986). Their model is given in Table 14-7. The differences in the upper mantle, where both studies have their highest resolution, are probably due to regional differences. The differences in the lower mantle probably reflect the intrinsic uncertainty in Q with available data.

The study of Q is in its infancy. The results given in this section are very preliminary. The variation of Q with frequency and the lateral variations are very uncertain. Even the average radial variation is uncertain because of the trade-offs between frequency and depth when inverting surface waves and free oscillations.

TABLE 14-7
 Q_s Model for the Eurasian Shield

Depth (km)	Q_s			
	0.01 Hz	0.1 Hz	1 Hz	10 Hz
50-100	216	246	365	665
100	216	246	365	665
150	123	138	200	380
200	123	138	200	380
250	123	138	530	950
350	123	356	530	950
425	307	356	530	950
659	307	356	530	950
660	565	860	2145	5825
1000	565	860	2145	5825
1571	580	1055	3860	16,155
2891	580	1055	3860	16,155

Der and others (1986).

General References

Anderson, D. L. (1967) The anelasticity of the mantle, *Geophys. J. R. Astr. Soc.*, 14, 135-164.

Anderson, D. L. and J. W. Given (1982) Absorption band Q model for the Earth, *J. Geophys. Res.*, 87, 3893-3904.

Anderson, D. L., H. Kanamori, R. Hart and H. Liu (1977) The Earth as a seismic absorption band, *Science*, 196, 1104-1106.

Anderson, D. L. and J. B. Minster (1979) The frequency dependence of Q in the Earth and implications for mantle rheology and Chandler wobble, *Geophys. J. R. Astron. Soc.*, 58, 431-440.

Friedel, J. (1964) *Dislocations*, Addison-Wesley.

Goetze, C. (1977) A brief summary of our present day understanding of the effect of volatiles and partial melt on the mechanical properties of the upper mantle. In *High-Pressure Research* (M. Manghnani and S. Akimoto, eds.), 3-23, Academic Press, New York.

Hirth, J. P. and J. Lothe (1968) *Theory of dislocations*, McGraw-Hill, New York, 780 pp.

Jackson, D. D. and D. L. Anderson (1970) Physical mechanisms of seismic wave attenuation. *Rev. Geophys.*, 8, 1-63.

Kanamori, H. and D. L. Anderson (1977) Importance of physical dispersion in surface-wave and free-oscillation problems; a review, *Rev. Geophys. Space Phys.*, 15, 105-112.

Minster, B. and D. L. Anderson (1981) A model of dislocation-controlled rheology for the mantle, *Phil. Trans. Roy. Soc. Lond. A*, 299, 319-356.

Nowick, A. S. and B. S. Berry (1972) *Anelastic Relaxation in Crystalline Solids*, Academic Press, New York, 677 pp.

Stevenson, D. (1983) Anomalous bulk viscosity of two-phase liquids and implications for planetary interiors, *J. Geophys. Res.*, 88, 2445-2455.

Stocker, R. and M. Ashby (1973) On the rheology of the upper mantle, *Rev. Geophys. Space Phys.*, 11, 391-426.

Van Bueren, H. (1960) *Imperfections in crystals*, North-Holland, Amsterdam, 676 pp.

Weertman, J. (1968) Dislocation climb theory of steady-state creep, *Trans. Amer. Soc. Metals*, 61, 681-694.

References

Anderson, D. L. (1966) Earth's viscosity, *Science*, 151, 321-322.

Anderson, D. L. (1980) Bulk attenuation in the Earth and viscosity of the core, *Nature*, 285, 204-207.

Anderson, D. L. and C. Archambeau (1964) The anelasticity of the Earth, *J. Geophys. Res.*, 69, 2071.

Anderson, D. L., A. Ben-Menahem and C. B. Archambeau (1965) Attenuation of seismic energy in the upper mantle, *J. Geophys. Res.*, 70, 1441-1448.

Anderson, D. L. and J. Given (1982) Absorption band Q model for the Earth, *J. Geophys. Res.*, 87, 3893-3904.

Anderson, D. L. and R. S. Hart (1979) Q of the Earth, *J. Geophys. Res.*, 83, 5869-5882.

- Anderson, D. L. and J. B. Minster (1979) The frequency dependence of Q in the Earth and implications for mantle rheology and Chandler wobble. *Geophys. J. R. Astr. Soc.*, **58**, 431–440.
- Anderson, D. L. and J. B. Minster (1980) Seismic velocity, attenuation and rheology of the upper mantle. In *Source Mechanism and Earthquake Prediction* (C. J. Allegre, ed.), 13–22, Centre national de la recherche scientifique, Paris.
- Anderson, D. L. and C. G. Sammis (1970) Partial melting in the upper mantle, *Phys. Earth Planet. Inter.*, **3**, 41–50.
- Ashby, M. F. and R. A. Verall (1978) Micromechanisms in flow and fracture, and their relevance to the rheology of the upper mantle, *Phil. Trans. R. Soc. Lond. A* **288**, 59–95.
- Berckhemer, H., F. Auer and J. Drisler (1979) High-temperature anelasticity and elasticity of mantle peridotite, *Phys. Earth Planet. Inter.*, **20**, 48–59.
- Berckhemer, H., W. Kampfmann, E. Aulbach and H. Schmeling (1982) Shear modulus and Q of forsterite and dunite near partial melting from forced oscillation experiments *Phys. Earth Planet. Inter.*, **29**, 30–41.
- Budiansky, B. and R. O'Connell (1980) *Solid Earth Geophys. Geotechn.*, AMD 42, Amer. Soc. Mech. Eng. 1980.
- Der, Z. A., A. C. Lees and V. F. Cormier (1986) *Geophys. J. Roy. Astron. Soc.*, **87**, 1103–1112.
- Flinn, J., P. Gupta and T. Litovitz (1974) *J. Chem. Phys.* **60**, 4390.
- Goetze, C. (1978) The mechanisms of creep in olivine, *Phil. Trans. R. Soc. Lond. A*, **288**, 99–119.
- Goetze, C. and W. F. Brace (1972) Laboratory observations of high temperature rheology of rocks, *Tectonophysics*, **12**, 583–600.
- Goetze, C. and D. L. Kohlstedt (1973) Laboratory study of dislocation climb and diffusion in olivine, *J. Geophys. Res.*, **78**, 5961–5971.
- Gutenberg, B. (1957) The "boundary" of the Earth's inner core, *Trans. Am. Geophys. Un.*, **38**, 750–753.
- Heinz, D. L., R. Jeanloz and R. J. O'Connell (1982) Bulk attenuation in a polycrystalline Earth, *J. Geophys. Res.*, **87**, 7772–7778.
- Hirth, J. and J. Lothe (1968) *Theory of Dislocations*, McGraw-Hill, New York, 780 pp.
- Jackson, D. (1969) Grain boundary relaxation and the attenuation of seismic waves, Thesis, M.I.T., Cambridge, Mass.
- Jaoul, O., C. Froideveaux and M. Poumellec (1979) Atomic diffusion of ^{18}O and ^{30}Si in forsterite: Implication for the high temperature creep mechanism, Abstract, I.U.G.G. XVII General Assembly, Canberra, Australia.
- Jeffreys, H. (1958) Rock creep, *Mon. Nat. R. Astr. Soc.*, **118**, 14–17.
- Jeffreys, H. (1965) *Nature*, **208**, 675.
- Jeffreys, H. (1970) *The Earth*, 5th ed., Cambridge University Press, London.
- Jeffreys, H. and S. Crampin (1970) On the modified Lomnitz law of damping, *Mon. Not. R. Astr. Soc.*, **147**, 295–301.
- Kampfmann, W. and H. Berckhemer (1985) High temperature experiments on the elastic and anelastic behaviour of magmatic rocks, *Phys. Earth Planet. Inter.*, **40**, 223–247.
- Kohlstedt, D. L. (1979) Creep behavior of mantle minerals, Abstract, I.U.G.G. XVII General Assembly, Canberra, Australia.
- Kohlstedt, D. L. and C. Goetze (1974) Low-stress high-temperature creep in olivine single crystals, *J. Geophys. Res.*, **79**, 2045–2051.
- Mavko, G. and A. Nur (1975) Melt squirt in the asthenosphere, *J. Geophys. Res.*, **80**, 1444–1448.
- Minster, J. B. and D. L. Anderson (1981) A model of dislocation-controlled rheology for the mantle, *Phil. Trans. Roy. Soc. London*, **299**, 319–356.
- Misener, D. V. (1974) Cationic diffusion in olivine to 1400°C and 35 kbar, *Carnegie Instn. Wash. Publ.*, **634**, 117–129.
- Nur, A. (1971) Viscous phases in rocks and the low velocity zone, *J. Geophys. Res.*, **76**, 1270–1278.
- O'Connell, R. J. and B. Budiansky (1978) Measures of dissipation in viscoelastic media, *Geophys. Res. Lett.*, **5**, 5–8.
- Spetzler, H. and D. L. Anderson (1968) The effect of temperature and partial melting on velocity and attenuation in a simple binary system, *J. Geophys. Res.*, **73**, 6051–6060.
- Toomre, A. (1974) On the "nearly diurnal wobble" of the Earth, *Geophys. J. R. Astron. Soc.*, **38**, 335–348.
- Vaisnys, R. (1968) Propagation of acoustic waves through a system undergoing phase transformations, *J. Geophys. Res.*, **73**, 7675–7683.
- Walsh, J. B. (1969) New analysis of attenuation in partially melted rock, *J. Geophys. Res.*, **74**, 4333–4337.
- Woirgard, J. (1976) Modèle pour les pics de frottement interne observés à haute température sur les monocristaux. *Phil. Mag.*, **33**, 623–637.
- Zener, C. (1948) *Elasticity and Anelasticity of Metals*, University of Chicago Press, Chicago.